B. Siemon, D. Eberle, H.-J. Rehli,
W. Voß, J. Pielawa

Airborne Geophysical Investigation of Buried Valleys

Survey Area
Ellerbeker Rinne, Germany
2005/2006

Interreg IIIB Project: Ancient Groundwater Reservoirs in Buried Valleys – Sustainable Water Resources for the Future

BURVAL

BGR Bundesanstalt für Geowissenschaften und Rohstoffe

Bundesanstalt für Geowissenschaften und Rohstoffe
Federal Institute for Geosciences and Natural Resources

Airborne Geophysical Investigation of Buried Valleys

Survey Area: Ellerbeker Rinne, Germany

2005/2006

Technical Report on the Interreg IIIB Project

Ancient Groundwater Reservoirs in Buried Valleys – Sustainable Water Resources for the Future (BurVal)

The project is part-financed by the European Union

In Cooperation with

LANU
Landesamt für Natur und Umwelt
Schleswig-Holstein, Flintbek, Germany
BSU
Behörde für Stadtentwicklung
und Umwelt, Hamburg, Germany

Authors: Dr. B. Siemon
Dr. D. Eberle
H.-J. Rehli
W. Voß
J. Pielawa

Date: September 25, 2006

Table of contents

List of figures:

List of tables:

List of maps:

36. Anomalies of the total magnetic field (ΔT),
37. Concentration of Potassium (K),
38. Concentration of Thorium (Th),
39. Concentration of Uranium (U),
40. Stripped total count rate (TC),
41. Ground level exposure rate in μR/h.

List of vertical resistivity sections:

Survey 2005:

Tie lines:

1. VRS 1.9,
2. VRS 1.8,
3. VRS 2.9,
4. VRS 2.8,
5. VRS 3.9,
6. VRS 3.8,
7. VRS 4.9,
8. VRS 4.8,
9. VRS 5.9,
10. VRS 6.9

Lines:

11. VRS 70.1,
12. VRS 73.1,
13. VRS 76.1,
14. VRS 79.1,
15. VRS 82.1,
16. VRS 85.1,
17. VRS 88.1,
18. VRS 91.1,
19. VRS94.1,
20. VRS 97.1,
21. VRS 97.2,
22. VRS 100.1,
23. VRS 103.1,
24. VRS 106.1,
25. VRS 109.1,
26. VRS 112.1,
27. VRS 115.1,
28. VRS 118.1,
29. VRS 121.1,
30. VRS 121.2,
31. VRS 124.1,
32. VRS 124.2,
33. VRS 127.1,
34. VRS 127.2,
35. VRS 130.1,
36. VRS 133.1,
37. VRS 133.2,
38. VRS 136.1,
39. VRS 139.1,
40. VRS 142.1,
41. VRS 143.1,
42. VRS 143.2,
43. VRS 144.1,
44. VRS 144.2,

Survey 2006:

Lines:

45. VRS 201.1,
46. VRS 202.1,
47. VRS 203.1,
48. VRS 204.1,
49. VRS 205.1,
50. VRS 206.1,
51. VRS 207.1,
52. VRS 208.1,
53. VRS 209.1,
54. VRS 210.1,
55. VRS 211.1,
56. VRS 212.1,
57. VRS 213.1,
58. VRS 214.1,
59. VRS 215.1,
60. VRS 216.1,
61. VRS 217.1,
62. VRS 218.1,
63. VRS 219.1,
64. VRS 220.1,
65. VRS 221.1,
66. VRS 222.1,
67. VRS 223.1,
68. VRS 224.1,
69. VRS 225.1,
70. VRS 226.1,
71. VRS 227.1,
72. VRS 228.1,
73. VRS 229.1,
74. VRS 230.1,
75. VRS 231.1,
76. VRS 232.1,
77. VRS 233.1,
78. VRS 234.1,
79. VRS 235.1,
80. VRS 236.1,
81. VRS 237.1,
82. VRS 238.1,
83. VRS 239.1,
84. VRS 240.1,
85. VRS 241.1,
86. VRS 242.1,
87. VRS 243.1,
88. VRS 244.1,
89. VRS 245.1,
90. VRS 246.1,
91. VRS 247.1,
92. VRS 248.1,
93. VRS 249.1,
94. VRS 250.1,
95. VRS 251.1,
96. VRS 252.1,
97. VRS 253.1,
98. VRS 254.1,
99. VRS 255.1,
100. VRS 256.1,
101. VRS 257.1,
102. VRS 258.1,
103. VRS 259.1,
104. VRS 260.1,
105. VRS 261.1,
106. VRS 262.1,
107. VRS 263.1,
108. VRS 264.1,
109. VRS 265.1,
110. VRS 266.1,
111. VRS 267.1,
112. VRS 268.1,
113. VRS 269.1,
114. VRS 270.1,
115. VRS 271.1,
116. VRS 272.1

Abbreviations

°	degree
’	minute
%	per cent
1-D	one-dimensional
α,β,γ,a,b,g	stripping ratios
a	aircraft background
Ah	ampere hour
a.m.s.l.	above mean sea level
b	cosmic stripping factor
Bi	bismut
b.g.l.	below ground level
BGR	Bundesanstalt für Geowissenschaften und Rohstoffe
BSU	Behörde für Stadtentwicklung und Umwelt, Geologisches Landesamt Hamburg
BurVal	buried valleys
°C	degrees Celsius
C	concentration
C	cosmic channel count
cm	centimetre
cps	counts per second
Cs	cesium
©	copy right
δ	residual
Δ	difference
d_a	apparent depth
D_a	apparent distance
DEM	digital elevation model
DC	direct current
DGPS	Differential Global Positioning System
DGPS-Z	vertical DGPS component
E	east
E	ground level exposure rate
ED	European Datum
EM	electromagnetic(s)
e	base of the natural logarithm ($1/e \approx 0.37$)
ERDF	European Regional Development Fund
F	normal magnetic field
f	frequency
ft	feet
GBA	Geologische Bundesanstalt

GPS	Global Positioning System
h	bird altitude
h_e	effective height
HEM	helicopter electromagnetic(s)
Hz	hertz
i	counter
IAEA	International Atomic Energy Association
IAGA	International Association of Geomagnetism and Aeronomy
IGRF	International Geomagnetic Reference Field
K	potassium
kg	kilogram
kHz	kilohertz
km	kilometre
km²	square kilometre
km/h	kilometres per hour
LANU	Landesamt für Natur und Umwelt Schleswig-Holstein
L	litre
L/h	litres per hour
log	logarithm
lt	life time
m	metre
MAG	magnetics
mbar	millibar
MeV	mega electronic volts
mm	millimetre
m.s.l.	mean sea level
mV	millivolt
μ	adsorption value / attenuation coefficient
μR/h	microroentgens per hour
n	number of frequencies
N	north
N	background radiation
n, N	raw, corrected count rate
NaI	sodium iodid
nT	nanotesla
Ωm	ohm metre (Ohm*m)
P	barometric pressure
PC	personal computer
ppm	parts per million
Q	quadrature or out-of-phase component of the HEM data

R	inphase component of the HEM data
r	distance parameter
ρ	resistivity
ρ_a	apparent resistivity
S	south
S	sensitivity
s, sec	second
SCI	radiometrics (scintillometry)
STP	standard pressure and temperature
t	thickness (of a model layer)
t	time variable
t	corrected count rate
T	temperature
T, TMI	total magnetic field
ΔT	anomalies of the total magnetic field
Th	thorium
Tl	thallium
U	uranium
UTC	Coordinated Universal Time
UTM	Universal Transverse Mercator Projection
TC	total count
VRS	vertical resistivity section
V	volt
V_M	mean of diurnal variation
ΔV	diurnal (magnetic) variations
W	west
WGS	World Geodetic System
x,y,z	cartesian coordinates, z depth axis
z^*	centroid depth
ζ, λ	geographical coordinates (ζ = latitude, λ = longitude)

1. Summary

Buried valleys or sub-glacial melt-water drainage channels are subject of the project "Ancient groundwater reservoirs in buried valleys (BurVal) – sustainable water resources for the future" which has been jointly launched by several European partners in Germany, Denmark and The Netherlands in 2004. The project focuses mainly on groundwater reservoirs found in the shallow strata deposited during Quaternary Late Middle and Upper Pleistocene times, which include three major Ice Ages, the Elsterian, Saalian and Weichselian glacial periods. The Quaternary morphology of this area is dominated by several buried channels. Their origin is attributed to sub-glacial melt-water transport incising the underlying sedimentary strata during periods of glacial coverage. Such channels were commonly developed in the melting zones of the glaciers. After the retreat of the glaciers, the ground floor topography was filled by marine and glacio-marine sediments, often in form of fine grain sediments like clays and silts.

The aims of the BurVal project can be summarized to deliver knowledge and understanding of the structural and hydrological properties of deeper groundwater resources found in buried valleys, to focus on the vulnerability of surface contamination or other human impacts, and to investigate interactions with other water reservoirs and saltwater intrusions. This should lead to the development of spatial planning strategies that take these ancient groundwater reservoirs into account. The project is part-financed by the European Union (Interreg IIIB North Sea Programme of the European Regional Development Fund - ERDF) and focuses on six special project areas in Germany, Denmark and The Netherlands. Details can be found on the web site of the project (http://www.burval.org).

In charge of the German Landesamt für Natur und Umwelt des Landes Schleswig-Holstein (LANU) and Behörde für Stadtentwicklung und Umwelt, Geologisches Landesamt Hamburg (BSU), one of the six pilot projects is carried out in the Ellerbeker Rinne area, Germany, where a buried valley stretches from the small town Barmstedt in southern Schleswig-Holstein in south-east direction at a length of about 25 km to the downtown area of the Free and Hanseatic City of Hamburg. A helicopter-borne survey, split in two parts, was conducted by the airborne group of the German Federal Institute for Geosciences and Natural Resources (BGR) in April 2005 and in May 2006. The airborne survey comprises a 8-12 km by 28 km wide area from about 9°40'E to 9°59'E and 53°38'N to 53°55'N. With 7 flights 99 ENE–WSW profile lines and 6 NNW–SSE tie–lines were flown, totalling about 893 line-km. The nominal flight-line spacing was 400/600 m for the profile lines and 2000 m for the tie-lines.

The BGR helicopter-borne geophysical system includes five-frequency electromagnetics (HEM), magnetics (MAG) and gamma-ray spectrometry (SCI). The electromagnetic system provides information about the distribution of electrical conductivity in the earth down to a maximum depth of 150 m. The intensity of the earth's total magnetic field is measured with a magnetometer. Magnetic anomalies may have deep sources as well as shallow ones. The intensity of the gamma radiation is registered by a gamma-ray spectrometer. The radiation measured is mainly emitted from the elements thorium, uranium, and potassium. The origin of this radiation is normally close to the earth's surface.

The helicopter-borne system consists of the BGR-helicopter, the geophysical equipment and electronic equipment for navigation. The HEM and MAG sensors, the GPS antenna and a laser altimeter are installed inside a towed tube, called the bird. The navigation instruments and the gamma-ray spectrometer are mounted in the helicopter. A ground base station records the time-variant data required to correct the airborne data.

The survey altitudes of the sensors are normally 30–40 m for electromagnetics and magnetics and 70–80 m for gamma-ray spectrometry. HEM and MAG data are recorded 10 times per second during a survey flight and SCI data is recorded once per second. At an aircraft speed of about 140–150 km/h, this leads to mean sampling intervals of about 4 m and 40 m, respectively.

The collected geophysical data and the corresponding positioning data are stored on a ZIP disk during the flight. The digital data is checked immediately after the flight. Further processing of all survey data, including the data of the simultaneously operating base station which records the variations of the total magnetic intensity and the variations of the atmospheric pressure, take place in the field and finally at BGR in Hannover.

This “Technical Report” describes the survey operations and the survey equipment used, as well as the data processing and the presentation of the results as vertical resistivity sections and thematic maps. The processed data, the thematic maps and the vertical sections are stored on CD-ROMs, accompanying this report.

2. Introduction

Buried valleys or sub-glacial melt-water drainage channels are subject of the project "Ancient groundwater reservoirs in buried valleys (BurVal) – sustainable water resources for the future". The project focuses mainly on groundwater reservoirs found in the shallowest strata deposited during Quaternary Late Middle and Upper Pleistocene times, which include three major Ice Ages, the Elsterian, Saalian and Weichselian glacial periods. The Quaternary morphology of this area is dominated by several buried channels. Their origin is attributed to sub-glacial melt-water transport incising the underlying sedimentary strata during periods of glacial coverage (Huuse & Lykke-Andersen, 2000: Huuse et al. 2003). Such channels were commonly developed in the melting zones of the glaciers (Boulton et al., 1995; Boulton & Caban, 1995). After the retreat of the glaciers, the ground floor topography was filled by marine and glacio-marine sediments, often in form of fine grain sediments like clays and silts (Gausland, 1998; Huuse & Lykke-Andersen, 2000).

Today, these ancient valleys are buried by Quaternary sediments. Buried valleys are often important groundwater reservoirs. Valleys located close to the coast are threatened by saltwater intrusions while valleys beneath farming land might be contaminated by deep penetrating nitrate. As it is important to investigate buried valleys, the project BurVal has been jointly launched by several European partners in Germany, Denmark and The Netherlands in 2004.

The aims of BurVal are to deliver knowledge and understanding of the structural and hydrological properties of deeper groundwater resources found in buried valleys, to focus on the vulnerability of surface contamination or other human impacts, and to investigate interactions with other water reservoirs and saltwater intrusions. This should lead to the development of spatial planning strategies that take these ancient groundwater reservoirs into account. The project is part-financed by the European Union (Interreg IIIB North Sea Programme of the European Re-

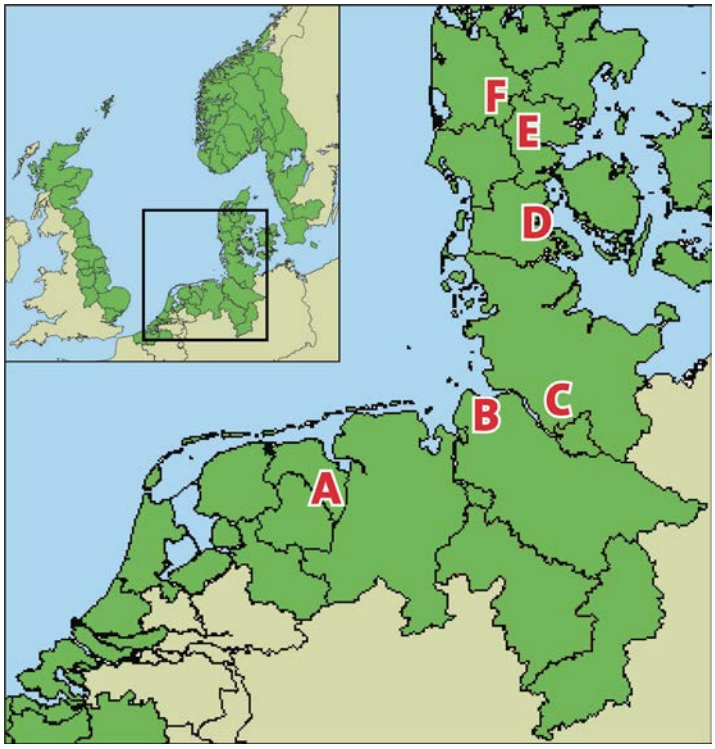

Fig. 1: *Regions (dark green) funded by the Interreg IIIB North Sea Programme of the European Regional Development Fund (ERDF) and project areas: A: Groningen Valley, Germany, B: Cuxhaven Valley, Germany, C: Ellerbek Valley, Germany, D: Rødekro Valley, Denmark, E: Tyrsting Valley, Denmark, and F: Bording Valley, Denmark*

gional Development Fund – ERDF) and focuses on six special project areas in Germany, Denmark and The Netherlands. Details can be found on the web site of the project (http://www.burval.org).

One of the six pilot projects is carried out in the Ellerbeker Rinne area, Germany, where a buried valley stretches from the small town Barmstedt in southern Schleswig-Holstein in south-east direction at a length of about 25 km to the downtown area of the Free and Hanseatic City of Hamburg (C in Fig. 1). The water reservoir of this valley is used by the Hamburger Wasserwerke and the Pinneberger Wasserwerke. Drillings reveal that the composition of the aquifer in the valley shows distinct lateral variations from medium to coarse sands in the southern part to fine sand to silt in the northern part. That means that the yield of the aquifer is high in the south and low in the north. The aquifer is covered with mica clay (Lauenburger Ton). In the area of Tangstedt (about 5 km NE of Pinneberg) the Ellerbeker Rinne is crossed by another, probably younger, valley. In this area the covering mica clay is replaced by boulder till.

A helicopter-borne survey, split in two parts, was conducted by the airborne group of the German Federal Institute for Geosciences and Natural Resources (BGR) in April 2005 and in Mai 2006. As the valley crosses the boundary between two German federal states, both the Landesamt für Natur und Umwelt des Landes Schleswig-Holstein (LANU) and Behörde für Stadtentwicklung und Umwelt, Geologisches Landesamt Hamburg (BSU) are responsible for the coordination of the measurements and the interpretation of the diverse data sets.

This “Technical Report” describes the survey operations and the survey equipment in use, as well as the data processing and the presentation of the results as vertical resistivity sections and thematic maps. The processed data, the thematic maps and the vertical sections are stored in a CD-ROM accompanying this report.

3. Airborne Survey

3.1. Ellerbeker Rinne Survey Area

Four of the six pilot areas have been surveyed by BGR using its helicopter-borne survey system. The Ellerbeker Rinne survey area is situated to the north-east of the Free and Hanseatic City of Hamburg, Germany. It comprises a 8-12 km by 28 km wide area from about 9°40'E to 9°59'E and 53°38'N to 53°55'N. A map of the survey area (red dots) is shown in **Fig. 2**, which also shows the boundary (dashed black line) of the 1: 50,000 topographic map used to present the geophysical results.

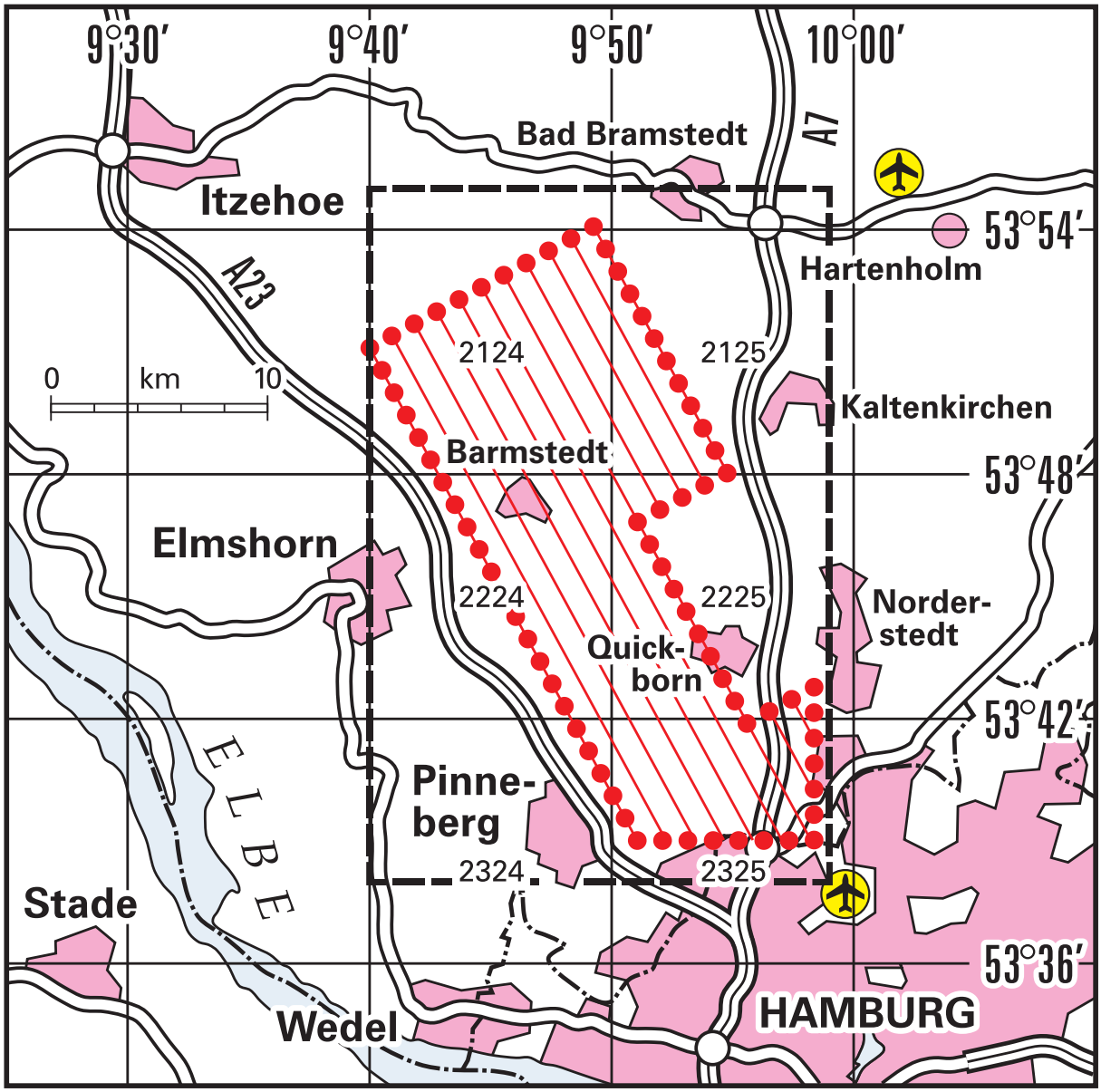

Fig. 2: *Ellerbeker Rinne survey area (red dots) and boundary of the 1:50,000 topographic map (dashed black line)*

An area of approximately 280 km² was surveyed with 7 flights on April 19–20, 2005 and May 16–19, 2006. There were 99 ENE–WSW profile lines and 6 NNW–SSE tie–lines flown, totalling about 893 line-km. The nominal flight-line spacing was 600 m in 2005 and 400 m in 2006 for the profile lines and 2000 m for the tie-lines. As a new HEM system has to be used for the survey in 2006, it covers the entire survey area but without tie-lines. The survey flights commenced from Hartenholm airport (32 m a.m.s.l.). The survey parameters are given in **Table 1**.

Table 1: *Survey parameters for the Ellerbeker Rinne survey area*

BGR area no.	111
Field period	April 19–20, 2005 May 16–19, 2006
Size of survey area	280 km^2
Total length of survey lines	893 km
Number of survey flights	7
Flight numbers	11100–11107
Mean flight altitude of the EM sensor above ground	50 m
Speed during survey flight	100–170 km/h
Number of profile-line flights	6
Number of profile lines	99 (106)
Profile-line lengths	9-12 km
Profile-line directions (angle to N)	ENE–WSW (28° / 208°)
Profile-line spacing	400/600 m
Number of tie-line flights	1
Number of tie-lines	6 (10)
Tie-line lengths	7–11 km
Tie-line directions (angle to N)	NNW–SSE (118° / 298°)
Tie-line spacing	2000 m

The survey had to be split into two parts due to technical problems with the helicopter in April 2005. As the helicopter had been shipped to Banda Aceh, Indonesia, in spring 2005 for several months, the completion of the survey could not commence until spring 2006. The lines flown primarily northwards or eastwards are normally given an even profile number, while the ones flown in the opposite directions are odd numbered. The profile lines have the extension ".1" (after the profile number) or ".2" for split lines, and the tie-lines have the extension ".9" or ".8" for split lines. Details of the survey flights are given in **Appendix I**.

The average altitude of the helicopter was 90 m above ground level within the survey area. During a survey flight, particularly before the first and after the last profile, the altitude was increased to >350 m to check the calibration of the HEM system far from any disturbing influences.

3.2. The BGR Airborne Geophysical System

BGR's airborne geophysical system simultaneously records the electromagnetic, magnetic, and gamma-ray spectrometry data. The geophysical instrumentation, the navigation and positioning systems, the analogue and digital recording units, as well as other equipment needed for the survey flights are integrated in one measuring system carried by a Sikorsky S–76B helicopter (**Fig. 3**). The HEM and MAG sensors, the GPS antenna and a laser altimeter are installed inside a towed tube, called the bird. The navigation instruments and the gamma-ray spectrometer are mounted in the helicopter. A ground base station records the time-variant data required to correct the airborne data.

Fig. 3: *BGR Sikorsky S-76B helicopter and bird on ground*

3.2.1. The Helicopter

The helicopter, a Sikorsky S-76B (see **Table 2**), was purchased in 1986 by the Federal Ministry for Economic Cooperation and Development and assigned to BGR, mainly for technical cooperation projects.

Table 2: *Specifications of the BGR helicopter D–HBGR*

Type	Sikorsky S-76B (Manufacturer: Sikorsky, USA)
Year of manufacture	1986
Engines	2 turbines Pratt & Whitney PT6B-36A with 1033 SHP (shaft horse power) for each
Maximum gross weight	11,700 pounds (5363 kg)
Maximum payload	3300 pounds (1500 kg)
Maximum flight duration	2¾ hours
Fuel consumption	350–400 L/h

3.2.2. The Geophysical Survey Systems

The units of the airborne geophysical systems are summarized in **Tables 3–8**.

Table 3: The geophysical survey systems

	The Geophysical Survey Systems	
Bird	**I. Five-Frequency Electromagnetic System (HEM)**	
	Function	Investigation of the underground electric conductivity down to a maximum depths of about 150 m
	System description	Digital electromagnetic system operating at five discrete frequencies; data are sampled 10 times per second. Five coplanar coil systems (transmitter (T), receiver (R), bucking, and calibration coils) are housed in a bird, about 10 m long and 0.5 m in diameter, made of Kevlar.
	Frequencies	375 Hz; 1778 Hz; 8510 Hz; 37,830 Hz; 128,500 Hz (2005) 387 Hz; 1820 Hz; 8225 Hz; 41,550 Hz; 133,200 Hz (2006)
	T-R coil separation	7.92 m; 7.91 m; 7.96 m; 8.03 m; 7.92 m (2005) 7.94 m; 7.93 m; 7.93 m; 7.91 m; 7.92 m (2006)
	Coil orientation	Horizontal coplanar for all frequencies
	Manufacturer	Fugro Airborne Surveys (FAS), Canada
	Type	DIGHEM$^{CP5\ DSP}$
	II. Magnetometer	
	Function	Recording of the total magnetic intensity of the earth
	System description	Optically pumped Cs-Magnetometer; 10 readings per second
	Location of sensor	Rear part of HEM bird
	Manufacturer	Sensor: Geometrics, USA; Console: FAS, Canada
	Type	Sensor: G-822A
Helicopter	**III. Gamma-Ray Spectrometer**	
	Function	Measurement of the energy spectrum of natural and man-induced gamma radiation within a range of 0 to 3 MeV
	System description	256-channel spectrometer, (a) 16.8 L NaI downward-looking detector crystal package and (b) 4.2 L NaI upward-looking crystal; self-stabilisation is achieved using (a) the thorium photo peak and (b) a cesium probe. Integration time: one second
	Manufacturer	Exploranium, Canada
	Type	Spectrometer: GR-820; Detector crystals: GPX-1024/256

During the second part of the survey in 2006 a digital five-frequency HEM system was used which frequencies and coil separations slightly differ from those of digital five-frequency HEM system used in 2005.

Table 4: *Navigation and positioning systems*

	Systems for Navigation and Positioning	
Helicopter	**Navigation System (DGPS)**	
	Function	On-line determination and display of the GPS navigational information required by the pilot: position of helicopter, deviation from the planned flight path, and distance to next way point. With the coordinates of the area corners, the profile direction [in degrees] and the spacing of the flight lines as input, the navigation computer calculates the coordinates of the starting and end points for all survey profiles. The planned profiles, the actual flight line, and the position of the helicopter are shown on a display. A separate display gives the pilot in graphical and digital form all the information used to fly a profile with the highest possible precision.
	System description	A 12-channel DGPS receiver with10 channels used to receive GPS signals and 2 channels used to receive the correction signals, e.g., from the OmniSTAR Service, makes the position data of the helicopter available to the navigation computer.
	Manufacturer	Navigation computer and display: AgNav, Canada DGPS receiver: CSI Wireless, Canada
	Type	Navigation computer: PNAV 2100 DGPS receiver: DGPS MAX
Bird	**Positioning System (DGPS)**	
	Function	Determination and recording of the geographic position and altitude of the HEM bird above mean sea level
	System description	A 12-channel DGPS from the same type used for the navigation system calculates the position of the bird 5 times per second. These position data are stored together with the other survey data.
	Manufacturer	CSI Wireless, Canada
	Type	DGPS MAX

Table 5: *Altimeters*

	Altimeters	
Helicopter	**Radar Altimeter**	
	Function	Recording of the altitude of the helicopter above ground level or above obstacles, such as forests and buildings
	System description	Radar impulses are transmitted from an antenna mounted at the bottom of the helicopter. The altitude of the helicopter is determined by evaluating the travel time of the impulses to the ground and back to the antenna. The radar altimeter responds to the very first reflections arriving from below, which means, for example, when the helicopter is over a forest the distance between the antenna and the treetops will be obtained instead of the distance to the ground. The radar altitude is recorded 10 times per second.
	Manufacturer	Sperry, USA
	Type	AA-200
	Barometric Altimeter	
	Function	Recording of the altitude of the helicopter above mean sea level
	System description	The air pressure is recorded and transformed into altitude values (in units of feet) and recorded 10 times per second
	Manufacturer	Rosemount, USA
	Type	1241A5B
Bird	**Laser Altimeter**	
	Function	Recording of the altitude of the HEM bird above ground with high precision
	System description	The laser altimeter hosted by the HEM bird emits impulses down to the ground. Evaluation of the travel time of impulses reflected at the ground surface provides the distance between the bird and the ground surface. Since the laser beam is extremely narrow it often penetrates the vegetation at the ground surface thus delivering the height of the HEM bird above ground surface. The laser altitude is recorded 10 times per second.
	Manufacturer	Riegl, Austria
	Type	LD90-31K

Table 6: *Data acquisition and recording systems*

	Data Acquisition and Recording Systems	
Helicopter	**Data Acquisition System**	
	Function	Digitizing the analogue signals, recording of the digital signals, organizing the selected data into data blocks, and transferring data blocks to digital and analogue data recorders
	System description	All signals to be recorded are managed by the data acquisition system. Sequence and intervals of data acquisition from the various sensors are adapted to the needs of data properties. Individual data are compressed into data blocks. Data blocks are then sent to digital (ZIP drive) and analogue data recorders during well defined time intervals. A digital display supports supervision of correct data transfer.
	Manufacturer	RMS, Canada
	Type	DAS 8
	Digital Data Recorder	
	Function	Recording of the data using a digital device
	System description	Data blocks containing ASCII and binary formatted data are recorded on a ZIP disk once a second.
	Manufacturer	RMS, modified by BGR
	Type	n/a
	Analogue Recorder	
	Function	Producing analogue records of all essential data during survey flight
	System description	Signals from up to 32 analogue and digital data channels are plotted by a high-resolution thermal printer onto 321 mm wide endless paper.
	Manufacturer	RMS, Canada
	Type	GR33A

Table 7: *Additional equipment*

	Additional Equipment	
Helicopter	**Video System**	
	Function	Recording of the flight track and monitoring of the movements of the HEM bird during take-off, landing and flight
	System description	The flight track is continuously filmed and taped using a video camera mounted on the floor of the helicopter. The pilot and the operator monitor the movements of the HEM bird via two screens placed in the cockpit and the instrument rack.
	Manufacturer	Camera: Pulnix, USA Video recorder: Toshiba, Japan
	Type	Camera: TMC-63M; Video recorder: V701 TO
	Central Power Unit	
	Basic principle	28 V DC on-board voltage of the helicopter filtered by a 24 Ah buffer battery is connected to a central power unit. From there it is distributed to the individual components of the system with fuses built-in to protect devices from overvoltage.
	Central Signal Distribution	
	System description	Distributing the analogue signals onto the digital recorder, visualizing the most important analogue and digital survey data.
	Instrument Rack	
	Characteristics	19” rack to mount all components of the airborne geophysical system. Shock absorbers between the base of the rack and a wood board which is firmly screwed to the floor of the helicopter minimize the transfer of vibrations originating from the rotor.

Table 8: *Base stations*

	Base Station	
Base station	**Magnetic and Barometric Base Station**	
	Function	Recording of the variations of the total magnetic intensity (TMI) and of the atmospheric pressure for corrections to be applied on some of the collected survey data
	System description	The base station is portable, weather-proof and equipped with own power supply. It serves to automatically record the variations of the TMI and atmospheric pressure. Routinely, one reading is taken per second. Since these readings have to be synchronized with the air-borne survey data, the GPS time of each reading is also recorded.
	Manufacturer	Base station: FAS, Canada Magnetometer: Sensor – Cs-Sensor H-8, Scintrex, Canada Barometer: MPXS4115A, Motorola, USA
	Type	CF1 Data Logger

3.3. Tasks and Function of the Airborne Geophysical System

A sketch of the BGR airborne geophysical system is shown in **Fig. 4**; a simplified block diagram of the survey system is shown in **Fig. 5**. The bird is connected to the helicopter by a cable of approximately 45 m length. Depending on the flight speed, the bird is towed about 41 m beneath the helicopter. This length of cable was chosen to avoid the influence of the helicopter on the highly sensitive magnetic and electromagnetic sensors.

The shell of the approximately 10-m-long cigar-shaped “bird” with a diameter of 0.5 m is made of Kevlar to obtain high flexural strength. This material has an extremely high mechanical stability and poor electric conductivity.

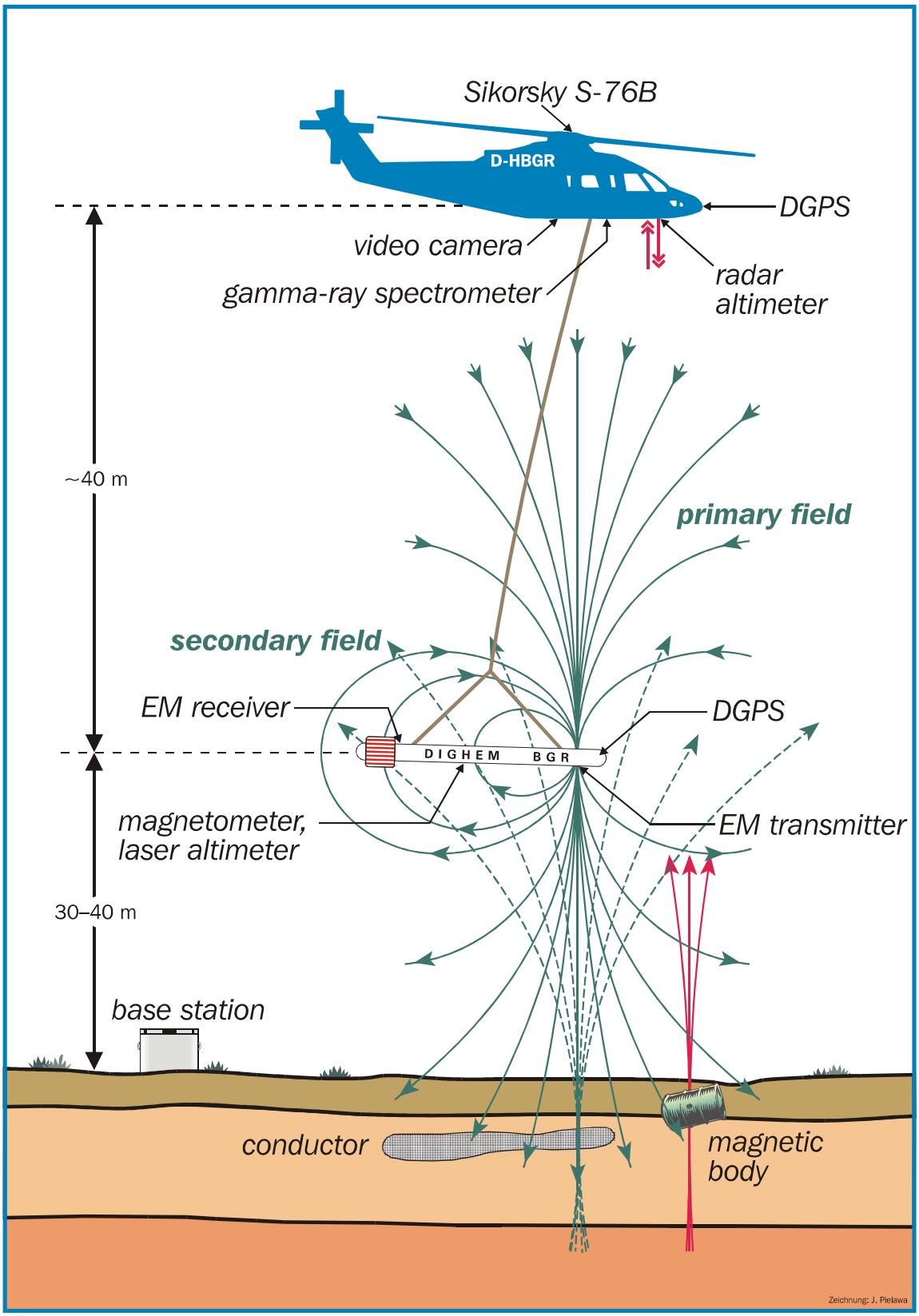

Fig. 4: *The airborne geophysical system*

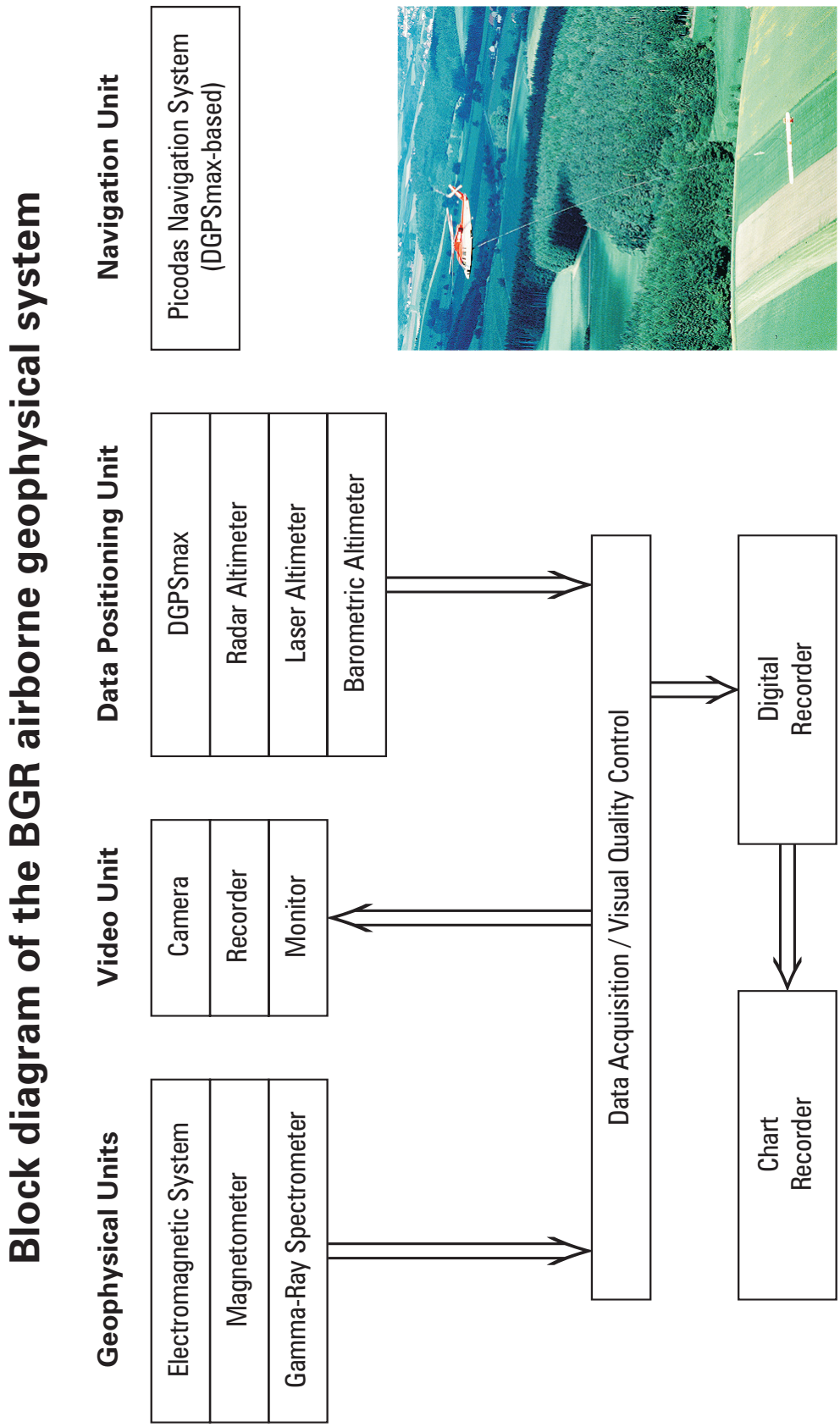

Fig. 5: *Block diagram of the airborne geophysical system*

3.3.1. Electromagnetics

The transmitter coils of the HEM system create sinusoidal magnetic fields at discrete frequencies. These primary fields induce eddy currents in electrically conducting earth. In turn, these currents generate magnetic fields, the secondary fields, which are detected by the receiver coils (**Fig. 4**). The strength and the phase shift of these very weak secondary fields depend on the electric conductivity in the subsurface, the frequency used, and the altitude of the system above ground level.

The HEM system uses separate coil systems (transmitter, receiver, bucking, and calibration coils installed horizontally and coplanar) for each of the five frequencies between 375/387.2 Hz and 128.5/133.2 kHz (**Table 3**). As the secondary fields are related to the primary fields at the receivers, which are compensated using bucking coils with exactly known specifications, relative units are useful. The unit ppm (parts per million) is used because the strength of the secondary field is much smaller than the strength of the primary field at the receiver coils. Internal calibration coils generate calibration signals in the receivers. These signals which ppm values are provided by the manufacturer are used to determine the conversion factors for the measured secondary field voltages.

The electrical conductivity (or its reciprocal: resistivity) can be calculated from amplitude and phase shift or from in-phase and out-of-phase components of the secondary field. Due to the electromagnetic skin effect, the electromagnetic fields are associated with different penetration depths for each of the frequencies used: The lower the frequency and the higher the resistivity, the greater the penetration depth. With the lowest frequency of 375 Hz currently used, investigation depths up to 150 m are obtainable under ideal conditions.

The HEM system is not only sensitive to the electrically conductive subsurface but also to anthropogenic objects like, e.g., buildings, metallic bodies, and electrical installations, which have influence on the data measured, particularly at lower frequencies. As the helicopter itself is such an object, the HEM system is installed in a rigid tube, called “bird” (**Table 3**), which is towed at a sufficiently large distance (about 40 m) underneath the helicopter.

3.3.2. Magnetics

The total intensity T of the earth’s magnetic field is measured with a highly sensitive cesium magnetometer. This magnetic field is composed of three parts: The total magnetic intensity field of the earth – with its minimum at the equator and its maximum at the poles – is overlain by anomalous magnetic fields from geogenic sources (e.g., magnetite-containing minerals and mineral deposits) as well as from fields of anthropogenic nature (buildings, industrial plants, waste deposits and others). The more general geogenic anomalies cover a larger area than anomalies resulting from anthropogenic sources, which are mostly of local nature.

The cesium sensor provides a signal with a frequency called the Larmor frequency, which is directly proportional to the total field intensity. The proportionality constant is 3.4986 Hz per nT. The operating range of the instrument is 20,000–100,000 nT.

Owing to the sensitivity of the cesium sensor, which determines the total magnetic field with a resolution of 0.01 nT, the sensor is installed in the middle of the bird, preferably far from the helicopter. The sensor is mounted so that it can be adjusted with respect to the flight line direction to get the maximum signal strength.

3.3.3. Gamma-Ray Spectrometry

BGR uses a standard spectrometer system consisting of four sodium iodide (NaI) crystals to detect the ground gamma radiation and one upward looking crystal to detect the radon radiation in the air. For geophysical investigations the count rates of the common terrestrial radioactive elements (or their isotopes and daughter products) Tl-208 (thorium series), Bi-214 (uranium series), K-40 (potassium) are of interest. The different distributions of these three elements in the ground are useful for geological mapping.

The spectrometer crystals are placed together in an aluminium box. Each crystal has a volume of approximately 4 L (10×10×40 cm). Incident gamma radiation is absorbed by the crystals and transformed into light impulses. These impulses are converted into electric impulses by a photomultiplier; the amplitudes of the electrical impulses are directly proportional to the energy of incident gamma radiation. Depending on their energy, the pulses are sorted into one of the 255 energy channels covering the entire energy spectrum from 0 to 3 MeV; channel 256 is provided for cosmic radiation between 3 and 6 MeV. Integrated over one second, gamma radiation in the energy windows for the total radiation, for potassium, uranium and thorium, as well as for each channel of the spectrum, is recorded. Energies and channels for the different radiation sources are shown in **Table 9**. The spectrometer is calibrated and stabilised against an internal standard. This is done for each of the four downward-looking crystals using the thorium peak. Shifts of the thorium peak (2.62 MeV) relative to the nominal value are identified and the gain of the photomultiplier of the respective crystal corrected automatically. A cesium probe is used to stabilize the gain of the upward looking crystal.

Table 9: *Radiation sources and corresponding spectrometer parameters*

Radiation Source	Energy Window in MeV	Peak Energy in MeV	Channel Range
Total count	0.41–2.81	—	34–233
Potassium (K-40)	1.37–1.57	1.46	115–131
Uranium (Bi-214)	1.66–1.86	1.76	139–155
Thorium (Tl-208)	2.41–2.81	2.62	202–233
Cosmic radiation	3.0–6.0	—	255

3.3.4. Navigation and Positioning

The navigation system (**Table 4**) provides the pilot with all the information necessary to carry out a survey flight. The navigation computer calculates the coordinates of the starting and the end points of all survey profiles from the coordinates of the corners of the survey area, the profile direction and the spacing of the flight lines. These profiles are shown on a display and the line being flown is highlighted.

The pilot obtains all the information required to fly this profile as accurately as possible from a second display. The most important information is the lateral deviation from this line. The deviation appears digitally in metres, as well as on a bar diagram. The navigation computer receives information about the position of the helicopter from a DGPS navigation receiver whose antenna is fixed outside on the helicopter. The error in the navigation data is less than 1–2 m.

The positioning system (**Table 4**) provides the coordinates of each and every geophysical measurement. A second DGPS navigation receiver is used for this purpose, whose antenna is fixed outside at the bird. The spatial positions of the sensors are determined from this positioning data. The error of the coordinates is also in the order of 1–2 m.

A radar altimeter attached to the bottom of the helicopter determines its altitude above the ground or above obstacles (e.g., large stands of trees and buildings) with a precision of ±3 m. The altitude is needed to process the radiometric data. A barometric altimeter is used to determine the altitude of the helicopter above mean sea level, but is employed only as a backup for the DGPS receivers. The altitude of the bird above the ground must be accurately known for the processing of the electromagnetic data and to generate a digital terrain model. A laser altimeter inside the bird provides this altitude with a precision of ±0.2 m. A further advantage of the laser altimeter, in addition to its precision, is the focused laser beam, which when above a forest often allows the distance to the surface to be determined and not only to the treetops, as is the case with the radar altimeter. The digital elevation model is derived from the elevation of the HEM bird in m a.m.s.l. minus the laser altitude. The altimeters are described in **Table 5**.

3.3.5. Data Recording

All the data are stored digitally on an IOMEGA ZIP disk during a survey flight (**Table 6**). The most important data channels are plotted on chart paper to enable continual checking of the data during the flight. Immediately after a flight, the analogue plots are checked more accurately in order to obtain an impression of the geophysical results, but also to detect any problems with the survey system. The digital data are transferred to a PC, checked and prepared for further processing.

3.3.6. Video System

A video camera is mounted in the bottom of the helicopter. Two monitors, one in the cockpit and one in the operator's rack, allow monitoring of the bird at take-off and landing and during the flight.

The video recording of the flight path is used to locate sources of anomalous or disturbed data on the ground. By including the GPS time and a record counter on the video record, the flight path can be correlated directly with the analogue and digital data.

3.3.7. Base Station

The total magnetic field of the earth is not constant and the temporal variations can range from milliseconds to many hours. The normal magnetic daily variations recorded during the surveys show peak-to-peak values from 20 nT to 100 nT. The atmospheric pressure also shows temporal variations.

The total magnetic field and the atmospheric pressure is recorded at a base station (**Table 7**) equipped with a magnetometer and a barometer. During a survey it is placed at a location with low magnetic disturbances. The daily variations are determined from the values collected for both parameters. They are used to correct the total magnetic field and barometric altitude measured during the flight. The airborne and base station data are correlated using the GPS time recorded by both devices.

4. Processing and Presentation of the Survey Data

The general objectives of the data processing may be summarized as follows:

- removal of noise and bias in the data;
- conversion of the data into physical parameters;
- presentation of the results as maps and vertical sections.

4.1. Processing Steps

The airborne geophysical data were verified in the field for plausibility and for correctness to determine whether a flight needed to be repeated. If the data is accepted, the subsequent processing include the following steps (see **Fig. 6**):

- coordinate transformation;
- removal of the tree-canopy effect;
- fixing of the ends of the profiles;
- removal of spiky data;
- reduction of high-frequency noise by digital filtering;
- conversion of the data to the desired geophysical parameters;
- levelling of the data;
- storage of survey data and geophysical parameters for each of the profiles;
- production of maps and vertical sections (only HEM).

The filed data processing and the calculation of the physical parameters for each method are described in more detail in the following chapters.

4.2. Field Data Processing

4.2.1. Data Handling

The main tasks of the field data processing are:

- check and correction (if necessary) of the binary flight data;
- splitting of the binary flight data file into ASCII parameter files;
- transformation of the GPS coordinates to local coordinates used for map production;
- combination of parameters necessary for the geophysical methods;
- storage of ASCII flight data files for three geophysical methods.

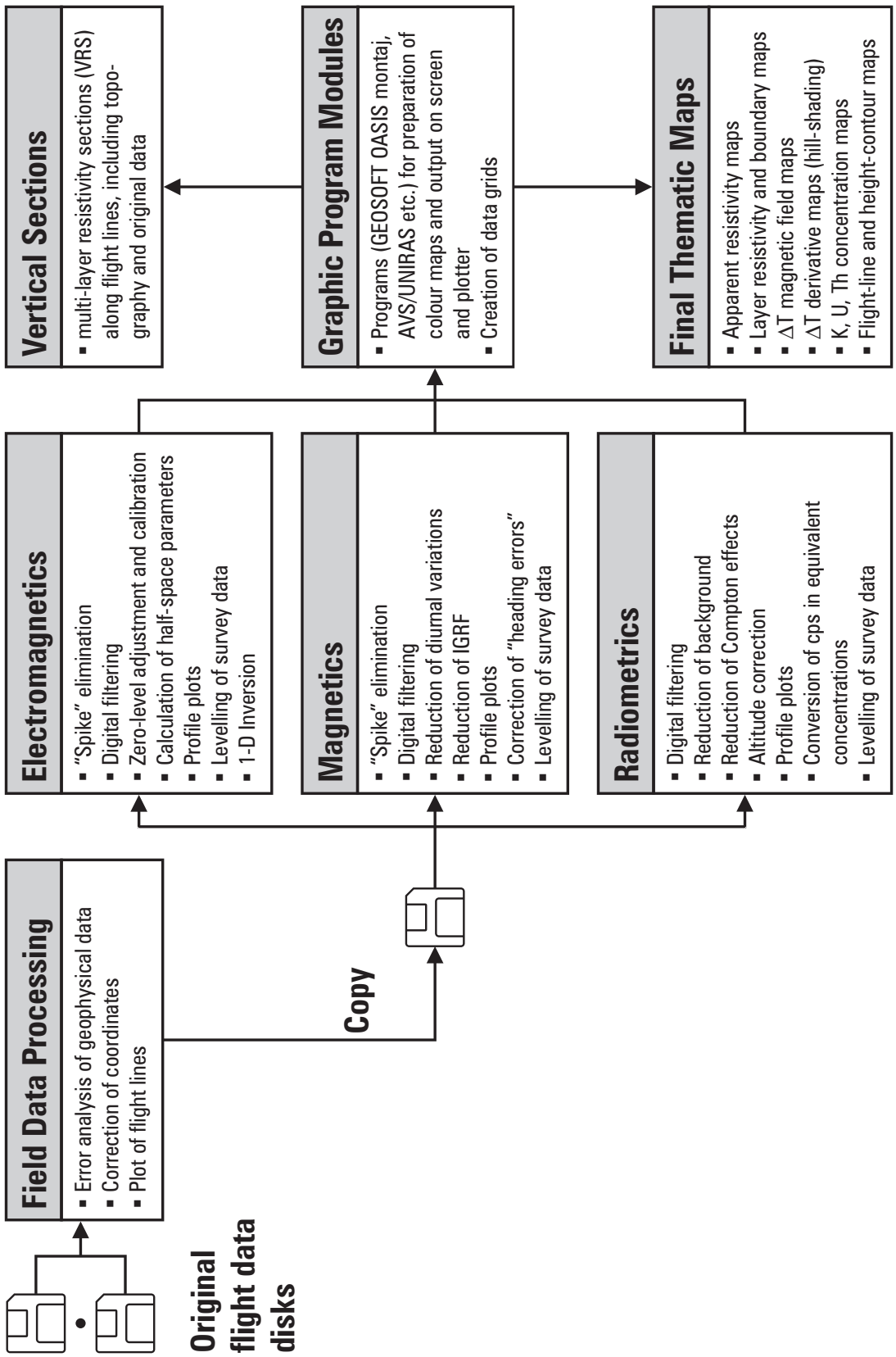

Fig. 6: *Block diagram of the data processing steps*

4.2.2. Tree-Canopy Effect

As the measurements of the radar altimeter (helicopter) and laser altimeter (bird) may be affected by the tree canopy or other reflectors, the distance between the helicopter containing the radiometric system or the bird containing the electromagnetic and magnetic systems and the ground is often not correctly measured resulting in radar and laser altitudes which are too low and topographic elevations which are too high (**Fig. 7**).

As the accuracy of the measurements of the laser altimeter is higher than those of the radar altimeter, first the radar altitude values are adjusted to the laser altitude values:

h_{radar} [m]= h_{radar} [mV] a + b

where

h_{radar} [m]	=	adjusted radar altitude (unit: m),
h_{radar} [V]	=	radar altitude (unit: V) measured by the altimeter,
a	=	conversion factor (unit: m/V) containing the unit conversion (4 mV/ft, 1 ft = 0.3048 m) and the laser altitude based correction factor (1.04),
b	=	averaged distance (unit: m) between the helicopter and the bird (including an offset in the radar altitude measurements), 2005: 47 m; 2006: 44 m.

Extreme laser altitudes are then replaced by adjusted radar altitudes. The topographic relief derived by the difference of GPS based bird elevation and laser altitude is used to correct the laser altitude using a combination of several checks and filter techniques (**Table 10**). First a noise filter is used to determine the areas where trees or other obstacles exist (high noise level, threshold: 0.3 m) or not (low noise level). Then a minimum filter is applied to the high-noise elevation data followed by a low pass filter eliminating all effects caused by single or small groups of trees. The effect of broad, dense forests, however, is not always removed sufficiently and has to be corrected manually. Afterwards, the laser altitude values are recalculated from the corrected topographic elevation values.

Table 10: *Filters used for the removal of the tree-canopy effect*

Type of filter	Filter parameters
Noise (normal distribution)	Window length: 5 points (about 20 m)
Minimum	Window length: 51 points (about 200 m)
Low pass	Window and cut-off wave length: 101 points (about 400 m)

4.3. Processing of the Electromagnetic Data

The conversion of the measured R and Q values (in mV), i.e., the real part (in-phase or 0°-phase) and the imaginary part (out-of-phase or 90°-phase), to secondary field values (in ppm) is done in four steps:

- verification of phase and gain, and correction if necessary;
- zero level determination and correction if necessary;
- conversion of the data using calibration factors;
- correction of erroneous data.

The apparent resistivities and the centroid depths are then derived from the values of the secondary fields for each individual frequency and 1-D inversion models are calculated for each survey point using the data of all (or selected) frequencies.

4.3.1. Calibration of the HEM System

The HEM system was calibrated on highly resistive ground by the manufacturer in Mountsberg Conservation Area, Canada, using well-defined external calibration coils. On the basis of these known values, the signals caused by internal calibration coils are determined in ppm.

At the beginning of each survey flight and at high flight altitude, phase and gain of the EM system are adjusted automatically for each frequency using internal calibration coils. Due to instrumental drift, the calibration has to be checked several times during the flight. The calibration signals (in V) caused by internal calibration coils are compared with known calibration signals in ppm (provided by the manufacturer), and phase shifts and gain correction factors are calculated (**Table 11**). Using these values and after zero levelling (see Section **4.3.2**) the raw data (in V) is phase shifted, if necessary, and then converted into ppm values.

Table 11: *Calibration factors of the HEM systems*

System	Frequency	External R, Q [ppm]	Correction factors Gain [%], phase [°]
2005	375	210, 205	2, 0.0
	1778	220, 225	-5, 0.0
	8510	220, 210	27, 0.0
	37,830	660, 660	0, 0.0
	128,500	560, 560	20, -50; -10, 18; -15, -5.5
2006	387.2	208, 208	-5, -1.5
	1820	170, 173	0, -0.7
	8225	141, 141	27, 0.0
	41,550	636, 638	0, 0.4
	133,200	977, 993	0, 2.0

As the highest-frequency data of the original 139.6 kHz frequency of the HEM system used until 2005 was very noisy due to interferences with the third frequency (8510 Hz), the highest system frequency has to be changed to 128.5 kHz. Unfortunately, this frequency change demands a re-calibration of the system, which could not be carried out up to now due to missing own calibration facilities. To overcome this problem, a flight over highly conductive North Sea water during the Brædstrup survey in Denmark has been used to check the calibration values. The evaluation of this data set yielded a set of phase and gain corrections used for the processing of the Ellerbeker Rinne HEM data collected in 2005. Enormous phase shifts occurred in the highest-frequency data for the first part of the survey, which were corrected by a trial and error procedure. Therefore, it is still uncertain if the system used until 2005 has been calibrated accurately enough. The second part of the survey was flown with a new system that was carefully adjusted on the basis of several flights over sea water of the Andaman Sea.

4.3.2. Zero-Level Determination

The zero levels of the HEM data are generally determined at flight altitudes >350 m several times during a survey flight because the ground response is negligible at this altitude, i.e., the secondary field should be close to zero. Zero-level reference points are set at such high-altitude profile segments, preferably where the signal is not noisy. Signals measured at these high altitudes may still contain some non-compensated parts of the primary fields generated by the HEM system. The zero level is obtained by linear interpolation of the picked values at adjacent zero level reference points. The zero-level picking has to be repeated because the zero level may drift caused by temperature changes.

This procedure enables to remove the long-term, quasi-linear drift. Short-term variations caused by temperature changes due to altitude variations, however, which occur particularly in the highest-frequency data, cannot be corrected successfully by this procedure. Therefore, additional reference points – also along the profiles at normal survey flight altitude – have to be determined where the secondary fields are small but not negligible. At these locations, the estimated half-space parameters are used to calculate the expected secondary field values, which then serve as local reference levels.

4.3.3. Data Correction

Noise from external sources (e.g., from radio transmitters, power lines) are eliminated from the HEM data by appropriate filtering or interpolation. Induction effects from buildings and other electrical installations (see Section **4.3.6**) or effects from strongly magnetized underground sources are normally not erased from the data.

4.3.4. Transformation of the Secondary Field Values into Half-Space Parameters

The calibrated values of the secondary field R and Q (in ppm) for all frequencies are converted (Siemon, 2001) to the parameters of a homogeneous half-space (**Fig. 7**),

- apparent resistivity ρ_a (Ωm) and
- apparent distance D_a (m) from the sensor to the top of the conducting half-space.

The calculated distance D_a may differ from the observed HEM sensor altitude (in m above ground), i.e., the top of the conducting half-space model need not coincide with the surface of the earth as determined by the altimeters. The difference between the two is defined as the apparent depth $d_a = D_a - h$. If d_a is positive, a resistive cover is assumed above the half-space. If d_a is negative, a conductive cover is assumed.

In addition to the apparent resistivity ρ_a and apparent distance D_a, the centroid depth z* can be determined. The centroid depth is a measure of the mean penetration of the induced underground currents. The resulting sounding curves, $\rho_a(z^*)$, provide the initial approximation of the vertical resistivity distribution.

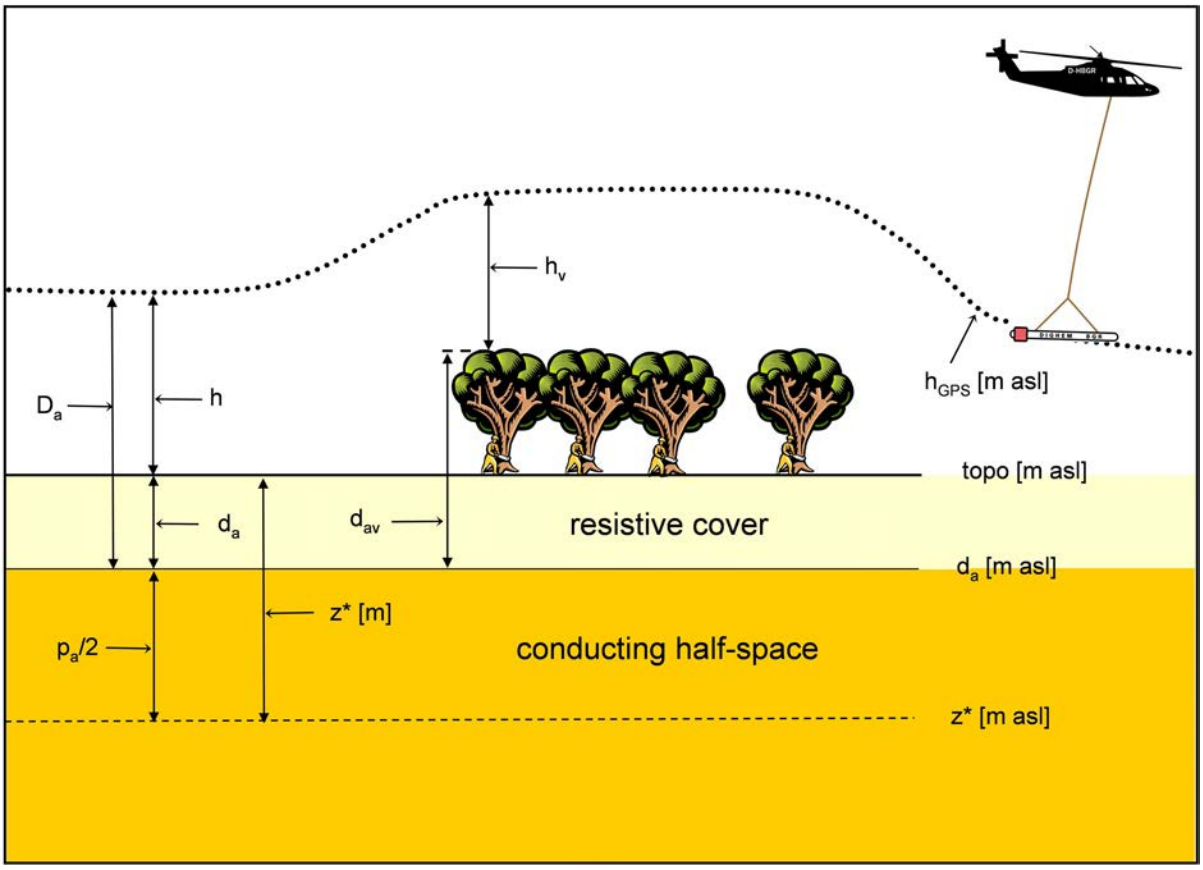

Fig. 7: *HEM inversion based on a homogeneous half-space or a layered half-space*

4.3.5. 1-D Inversion of the HEM Data

The model parameters of the 1-D inversion are the resistivities ρ and thicknesses t of a layered half-space (**Fig. 8**), where the thickness of the underlying half-space is assumed to be infinite. Marquardt's inversion procedure is used (Sengpiel and Siemon, 2000), which requires a starting model. This starting model is derived from the apparent resistivity vs. centroid depth values $(\rho_a, z^*)_i$, i=1,…,n. The standard model contains as many layers as frequencies used (n) plus a highly resistive cover layer. The layer resistivities are set equal to the apparent resistivities, the layer boundaries are chosen as the logarithmic mean of each two neighbouring centroid depth values. The thickness of the cover layer is derived from the apparent depth d_a of the highest fre-

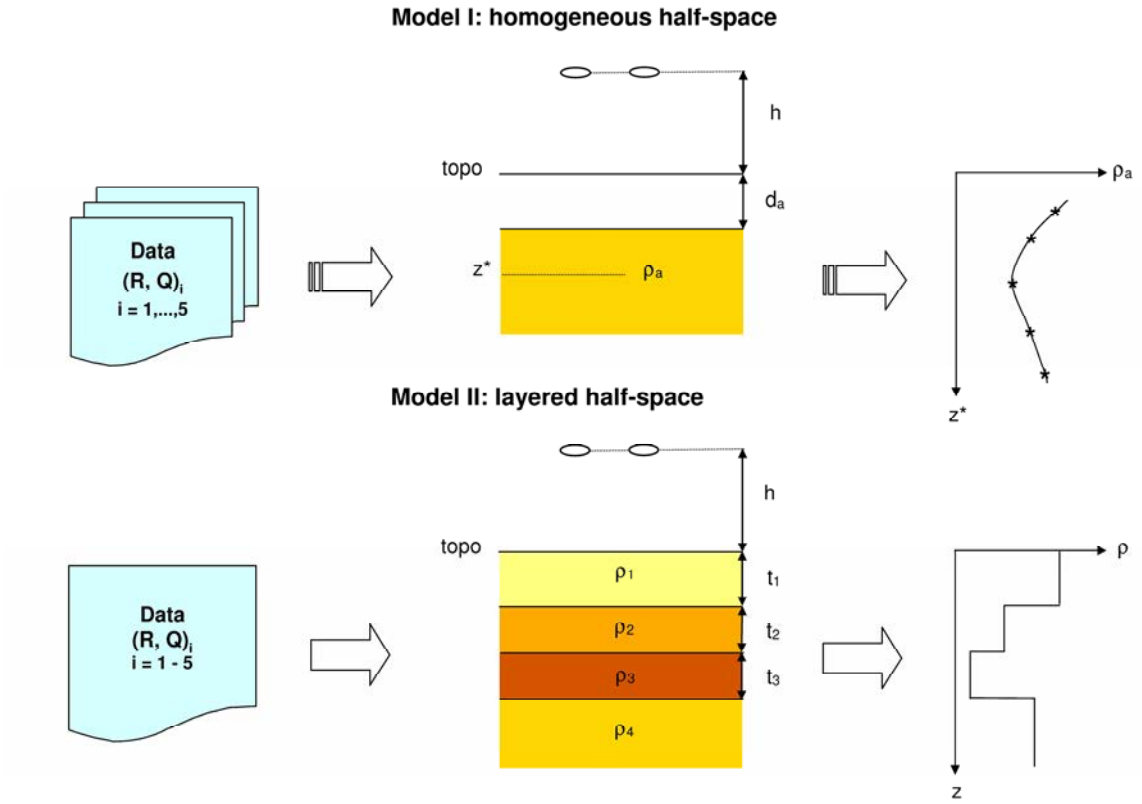

Fig. 8: *HEM inversion based on a homogeneous half-space or a layered half-space*

quency used for the inversion. If this apparent depth value is less than a given minimum depth value, the minimum depth value (e.g. 0.5 m) is used.

As the highest-frequency data may not be accurately calibrated (see Section **4.3.1**), the starting model used for the inversion was derived by combining the second layer and third layer, which were rather thin, i.e., a five-layer model was calculated (**Fig. 9**).

The inversion procedure is stopped when a given threshold is reached. This threshold is defined as the differential fit of the modelled data to the measured HEM data. We normally use a 10% threshold; i.e., the inversion stops when the enhancement of the fit is less than 10%.

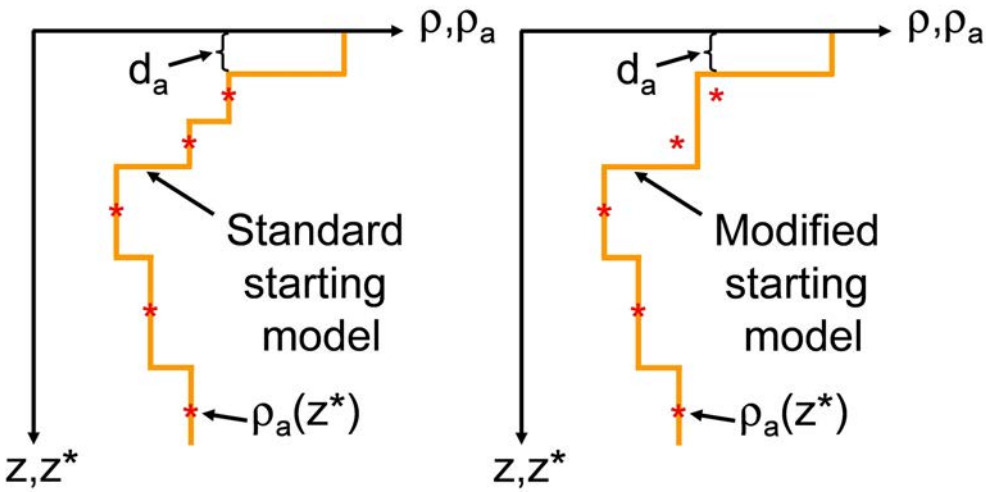

Fig. 9: *Calculation of the starting model from apparent resistivity, centroid depth, and apparent depth of a five-frequency HEM data set*

4.3.6. Effect of Anthropogenic Influences on the HEM Data

In addition to the geogenic contribution to the secondary fields measured over densely populated areas, there is often an anthropogenic contribution from buildings and electrical installations etc. Generally, these have little influence on the HEM data and the data can be corrected using the standard data processing tools. In some cases, e.g., large buildings with a high metal content, the anthropogenic components in the HEM data are no longer negligible. This can be seen particularly in the lower frequency data because the geogenic contribution to the secondary fields is comparatively smaller than at higher frequencies.

The anthropogenic influence lowers the calculated resistivity and associated depth. Low resistivities and low depths often correlate with villages or streets, particularly for the lower frequencies. When the 1-D resistivity models are placed side by side to construct a vertical resistivity section, the conducting layers appear to descend on either side of the anthropogenic source. Thus such three-dimensional effects cannot be interpreted adequately by the layered half-space model.

Anthropogenic influences can be detected in HEM data due to their typical form or by correlation with magnetic data. A topographic map of the survey area, an analysis of the video film or an on-site inspection can help identify such influences.

4.3.7. Statistical Levelling

In order to identify and to correct zero-level errors in the HEM data a grid based micro-levelling using GEOSOFT's OASIS-montaj software is applied to half-space parameters (log ρ_a and d_a).

First the half-space parameters of the 2006 survey were levelled which then served as a basis for the 2005 survey data. This procedure was chosen for two reasons: 1) The calibration of the HEM system used in 2005 was not as accurate as the calibration of the system used in 2006. 2) The system frequencies changed slightly and those of the new system were selected as reference.

Strong HEM anomalies are smoothed by two-dimensional lateral filtering of the micro-levelling procedure. Therefore, after micro-levelling, the half-space parameter values are converted to secondary field values which are compared with the corresponding unlevelled values. The strongly smoothed differences of the levelled and unlevelled values are assumed to characterize the zero-level errors and they are used to correct the HEM data without losing details. The levelling is done prior to the 1-D inversion of the HEM data.

4.3.8. Presentation of the Results

The HEM results are presented on maps and vertical resistivity sections (VRS). The maps are produced (see Section 4.5) for the half-space parameters, apparent resistivity and centroid depth. In addition, maps of the resistivity and depth (upper boundary) of the model layers 2-5 are derived from the 1-D inversion results after a weak levelling of the layer parameters. The latter are used to produce smooth 1-D inversion models from which the resistivity at certain depth levels (0-70 m b.s.l. at 5 m intervals) are picked and mapped. All the maps prepared from the results of this survey are listed in **Chapter 6**.

The VRS, also based on the 1-D inversion results, are produced for each of the survey lines. These vertical sections are constructed by placing the resistivity models for each sounding point along a survey profile next to each other using the topographic relief as base line (in m a.m.s.l.). The topographic elevation is derived from the EM system minus the laser altitudes. The altitude of the EM system with respect to m.s.l. is derived directly from the DGPS (DGPS-Z) readings or – if the GPS-Z data is not available – from the barometric altitude of the helicopter minus the mean effective cable length. The altitude of the EM sensor, information about the data processing, the fitting error of the inversion, and the HEM data, which are described in a legend, are plotted above the resistivity models.

4.4. Processing of the Magnetic Data

4.4.1. Magnetic Total Field

The earth's total magnetic field T at a point r and at a time t, e.g., measured with an airborne system, is the sum of the following parameters:

$$T(r,t) = F(r) + \Delta V(t) + \Delta T_e(r) + \delta(r,t)$$

where

$F(r)$	=	geomagnetic main field (IGRF = International Geomagnetic Reference Field),
$\Delta V(t)$	=	diurnal variations of the earth's magnetic field,
$\Delta T_e(r)$	=	the anomalous field in the survey area,
$\delta(r,t)$	=	small residual errors.

The anomalies of the total magnetic field $\Delta T_c(r)$ are of interest. While the IGRF F(r), which can be calculated from table values, and the diurnal variations $\Delta V(t)$, which are recorded at a local base station, can be subtracted from the measured total field, the residual errors $\delta(r,t)$ cannot be quantified independently. They are superposed on the anomalies $\Delta T_e(r)$, i.e., the derived ΔT values contain both the geogenic part and the disturbing anthropogenic part, whose sources (e.g. buildings) are mostly at the earth's surface or are caused by the helicopter itself.

4.4.2. IGRF Calculations

The IGRF (International Geomagnetic Reference Field) can be calculated for any point on and above the earth's surface at a specific time on the basis of spherical harmonic coefficients, which are updated every five years by the International Association of Geomagnetism and Aeronomy (IAGA, 1992). The IGRF 2005 of the particular epoch was calculated for the desired date at every point of the survey area (**Table 12**) using the geographical coordinates ζ and λ, (ζ = latitude, λ = longitude).

Table 12: *IGRF values for the Ellerbeker Rinne survey area*

Parameter	Values
IGRF	2005
Epoch	2006.4
Mean inclination /declination	+68.6° /+1.0°
Mean IGRF	49,417.0 nT
Mean value V_M / at base station	49,500.0 nT

4.4.3. Diurnal Variations

The base station for recording the time variant parts of the total magnetic field, the diurnal variations $\Delta V(t)$, was placed close to the airport. As usual, the mean value at the base station V_M, which is the mean value of the magnetic diurnal variations recorded during the survey, is used as the base for the local magnetic field and not the IGRF value at the site of the base station. This has the advantage that local anomalies can also be taken into consideration. The ΔV values, reduced by V_M, are subtracted from the recorded values during a survey flight. The recorded GPS times in the helicopter are synchronized with those recorded by the base station.

As no base-station data was available for the 2005 survey, only the magnetic data of the 2006 survey has been processed.

4.4.4. Statistical Levelling

In order to identify level errors in the data of the survey flights, the differences at the intersections of the flight lines with the tie-lines are determined and averaged. Afterwards, the correction values

are applied to the data. The correction values can be calculated for each profile line or for all of the profiles of a survey flight. The levelling also includes the elimination of so-called heading errors that occur as a result of the differing flight directions. If necessary, the line levelling is followed by a micro-levelling using GEOSOFT's OASIS-montaj software.

Due to the missing of the tie-lines for the 2006 survey, a statistical levelling of the flight lines was not possible. The correction of the heading error was carried out by determination of the mean value for ΔT of all flight lines flown in the same direction. The difference of both values was added to each ΔT value of every flight line. At least, the data of the total field was micro-levelled using GEOSOFT's OASIS-montaj software.

4.4.5. Presentation of the Results

The maps produced to display the magnetic anomaly data are listed in **Chapter 6**.

4.5. Processing of the Gamma-Ray Spectrometry Data

Corresponding to the recommendations of the IAEA (1979), the count rates of the radio elements potassium (K), uranium (U) and thorium (Th) recorded in the helicopter have to be converted into equivalent concentrations on the surface of the earth. The natural gamma radiation of the rocks and the soil is based mainly on these three sources. Moreover, the raw count rates include non-geogenic components, e.g., cosmic radiation and radiation from the helicopter itself. Radon, which varies considerably and can affect the interpretation because its radiation is detected by the uranium channel, is measured by the upward looking crystal and then corrected. As far as possible, these disturbing influences should be eliminated.

The following preparatory work and corrections are necessary:

- determination of cosmic and aircraft background count rates by flights over extensive bodies of water;
- evaluation of the absorption constants under survey conditions (atmospheric pressure and temperature) by means of ascending flights over land;
- reduction of the Compton effect, which occurs when the radiation penetrates the soil, the air and the sensor;
- correction of count rates recorded at different flight altitudes with respect to a standard flight altitude of 75 m in this case;
- conversion of the count rates from the standard flight altitude of 75 m to count rates on the ground;
- calculation of equivalent concentrations from the count rates on the ground.

4.5.1. Removing Cosmic and Aircraft Background

Cosmic radiation background is caused by high-energy cosmic ray particle interaction with the atmosphere. There is also background radiation from the immanent natural radioactivity of the

helicopter and its equipment. The background values for the gamma radiation had been derived once with the aid of a special flight about 50 km off-shore of Swakopmund, Namibia, by measurements over the Atlantic Ocean, where geogenic parts are negligible and "radon-free" conditions can be assumed. The measurements were taken at 1000, 3000, 5000, 6900, 7900, 8900, 9800, and 11500 ft a.m.s.l.. The measuring time at each altitude level was 10 minutes. The count rates were live time corrected according to the next chapter.

The cosmic and aircraft background correction will be done due to the following formula:

$$N = a + b * C$$

N = combined cosmic and aircraft background for each channel

a = aircraft background for each channel

b = cosmic stripping factor for each channel

C = filtered (low-pass) cosmic channel count

The values a and b are received for each channel K, U, Th, TC (total count) by linear regression of the filtered count rates in each spectral window of each altitude interval against the filtered cosmic channel count rates of each interval. The background values for the aircraft and the cosmic stripping factors are listed in **Table 13**.

Table 13: *Aircraft background a and cosmic stripping factor b*

Channel	Aircraft background a [counts per second]	Cosmic Stripping Factor b [counts per cosmic count]
TC	68.77	0.7771
K	8.32	0.0417
U	2.16	0.0363
Th	1.59	0.0338

4.5.2. Correcting Instrument Dead-Time/Live-Time Effects

The BGR spectrometer records a live time channel, so a live time correction can be easily performed due to:

$$N = n * 10^3 / lt$$

with

N = corrected count rate

n = raw recorded count rate

lt = recorded equipment live time in milliseconds

4.5.3. Adjustment of Radar Altimeter Data to Standard Temperature and Pressure

In order to apply the radiometric analysis techniques, it is necessary to convert actual conditions of the survey to "standard" conditions. This includes the adjustment of the measured ground clearance to standard temperature and pressure (STP-conditions). The corrected ground clearance value called "effective height" has the same mass of STP air between the ground and the helicopter as the actual one during data acquisition. Our program applies the correction as follows:

$$h_e = (h * P * 273) / (1013 * (T + 273))$$

h_e = effective height above ground level at STP (metres)

h = lightly filtered (despiked) radar altitude (metres) to remove the effect of sudden jumps

T = measured air temperature in °C (25°C assumed)

P = barometric pressure in mbar. P is derived from measured barometric altimeter data from the equation:

$P = 1013.32 * e^{(-h/8581)}$ where h is the filtered barometric altitude in metres.

4.5.4. Evaluation of Stripping Ratios on Calibration Pads and Stripping Correction

The stripping ratios had previously been recorded over calibration pads of the Geologische Bundesanstalt (GBA) in Vienna, Austria in 2003. The values are listed in **Table 14**.

Table 14: *Stripping ratios*

	Stripping Ratio	Value
U/Th	α	0.3044
K/Th	β	0.5128
K/U	γ	0.7361
Th/U	a	0.0767
Th/K	b	0.0043
U/K	g	0.0066

These ratios were computed using the PADWIN software.

The values of α, β, γ increase with altitude of the helicopter above ground level and have to be corrected on the base of STP equivalent altitude according to the following factors (see IAEA, 1991):

$$\alpha_e = \alpha + 0.00049 * h_e$$

$$\beta_e = \beta + 0.00065 * h_e$$

$$\gamma_e = \gamma + 0.00069 * h_e$$

h_e = equivalent height above ground level at STP in metres.

The stripping corrections are then applied to pre-processed and background-removed data as described in the next chapter.

4.5.5. Compton Correction

The dispersion of gamma rays by matter is called the Compton effect. This has the effect that part of the thorium radiation disperses into the energy ranges of the uranium and potassium windows. In similar manner uranium radiation disperses into the potassium channel. To obtain the net count rates of the particular channels, the stripping ratios have to be applied to the recorded and pre-processed data:

$$N_{K,K} = [N_{Th}(\alpha\gamma - \beta) + N_U(a\beta - \gamma) + N_K(1 - a\alpha)] / A$$

$$N_{U,U} = [N_{Th}(g\beta - \alpha) + N_U(1 - b\beta) + N_K(b\alpha - g)] / A$$

$$N_{Th,Th} = [N_{Th}(1 - g\gamma) + N_U(b\gamma - a) + N_K(ag - b)] / A$$

with

$$A = 1 - g\gamma - a(\alpha - g\beta) - b(\beta - \alpha\gamma)$$

where N_{Th}, N_K, N_U represent the background and STP corrected count rates, $N_{Th,Th}$, $N_{U,U}$, $N_{K,K}$ are the stripping corrected count rates, and α, β, γ, a, b, g the STP corrected stripping ratios. No Compton correction is applied to the total radiation values (see IAEA, 1991).

4.5.6. Height-Attenuation Reduction

The intensity of the gamma radiation from the surface of the earth decreases with increasing height of the sensor above ground because of absorption in the air. The energy-dependent absorption constant μ of the air is determined according to the procedure described in IAEA (1991). The absorption depends mainly on the density and humidity of the air. The value of μ is also influenced in the uranium channel by the fluctuating radon concentration in the air. Using these absorption values μ, the count rates N_m measured (background corrected and stripped) at the flight altitude h can be converted to the radiation intensities at a nominal survey altitude h_0 = 75 m.

$$N_s = N_m * e^{[-\mu \cdot (h_0 - h_e)]}$$

N_s = the count rate normalized to the nominal survey altitude h_0

N_m = the background corrected, stripped count rate at STP effective height h_e

μ = the attenuation coefficient for the spectral window

The values μ_{TC}, μ_K, μ_{Th}, μ_U had been evaluated over the Allensteig test range in Austria in 2003. BGR conducted a calibration flight at different heights over the calibration range. The values are tabulated in **Table 15**.

Table 15: *Height Attenuation Coefficient μ*

Window	Height Attenuation Coefficient μ (per metre at STP)
TC	–0.007438
K	–0.00875
U	–0.008868
Th	–0.006780

4.5.7. Calculation of Radio-Element Concentrations and Exposure Rate

The IAEA recommends converting the count rates for the three gamma radio elements into surface concentrations. The advantage of this is that the results of the measurements with different instruments (e.g., with different crystal volumes) can be compared with each other. The calculated count rates at ground level are converted into apparent concentrations of the three radio elements K (in %), U and Th (both in ppm) at ground surface using calibration factors. These factors were determined on the calibration range Allensteig in Austria. Following the IAEA recommendations, the total radiation is referenced by the ground level exposure rate. The equivalent concentrations refer to an infinitely extended and permanently radiating plane. They may differ from the actual concentrations of the elements ground surface, especially if the areas of radiation are distributed irregularly. Over dense and extensive forests the count rates are generally too small because of absorption by biomass and underestimation of the radar altitude, which reflects the distance from the helicopter to the tree canopy instead of the distance to the ground level.

At the Alleinsteig test range the concentrations of K, Th and U are known. They are listed at **Table 16**.

Table 16: *Element concentrations at Allensteig/Austria*

Channel	Concentration
K	3.64 ± 0.47 %
U	4.55 ± 1.03 ppm
Th	29.00 ± 5.47 ppm

The conversion of count rates to apparent radio-element concentration follows the relation:

$$C = N_s/S$$

C = apparent concentration of the element (K in %, U in ppm, Th in ppm)

N_s = the count rate for each window (after height attenuation and stripping)

S = the broad source sensitivity for the spectral window (see **Table 9**)

The broad source sensitivities S are given in **Table 17** for the Allensteig area. The term apparent concentration refers to the concentration in the ground of the elements potassium (K), uranium (U) and thorium (Th).

Table 17: *Sensitivities at Allensteig/Austria*

Sensitivity
1 % K = 32.45 cps
1 ppm Th = 2.31 cps
1 ppm U = 3.58 cps

Finally, the ground level exposure rate is calculated as a function of the K, U, and Th concentrations:

$$E = 1.505 \cdot K + 0.653 \cdot U + 0.287 \cdot Th$$

E = ground level exposure rate [µR/h]

using the following conversions (IAEA, 1991, p. 52):

1 % K = 1.505 µR/h,
1 ppm U = 0.653 µR/h,
1 ppm Th = 0.287 µR/h.

4.5.8. Statistical Levelling

In order to correct levelling errors in the data from different survey lines, the equivalent concentrations are micro-levelled using GEOSOFT's OASIS-montaj software.

4.5.9. Presentation of the Results

The results of the gamma-ray survey are presented as maps of the equivalent concentrations of the radio elements potassium, uranium, and thorium and the ground level exposure rate. The maps produced to display the radiometric data are listed in **Chapter 6**.

4.6. Map Production with GEOSOFT Software

Coloured contour maps were produced for each parameter of interest. The topographic map described in **Chapter 5** was used as map base. The surveyed flight lines are plotted where the map scale is large enough to distinguish between them.

The grids for the geophysical thematic maps are produced using the software package GEOSOFT's OASIS-montaj. **Table 18** shows the grid parameters used for the Ellerbeker Rinne survey. The final maps including geophysical, topographical and legend information are prepared using the program CorelDRAW 12. Adobe Acrobat is used for preparing the PDF documents.

Table 18: *Grid parameters*

Parameter	Value
Gridding method	Minimum curvature
Grid size [m]	50
Search radius [m]	400
Cell extend beyond data	10
Log option	log ρ (else linear)

5. Cartographic Work

5.1. Topographic Maps

A topographic map was produced as the base map for all thematic maps displaying the airborne geophysical results. A scale of 1:50,000 was chosen for the survey area. A Gauss-Krüger coordinate grid, based on the Bessel ellipsoid, is included on the topographic maps. **Table 19** contains the corner coordinates of the map sheet.

Table 19: *Coordinates of the corners of the 1:50,000 Ellerbeker Rinne topographic map sheet*

Map corners	Geographic coordinates (Bessel ellipsoid)		Gauss-Krüger coordinates (Bessel ellipsoid)	
	Easting	Northing	Easting	Northing
SW	9°40’	53°38’	3544094.8	5944698.2
NW	9°40’	53°55’	3543798.8	5976229.2
NE	9°59’	53°55’	3564602.7	5976471.3
SE	9°59’	53°38’	3565039.3	5944941.1

The map is based on the raster data of the »Topographische Karte 1:50,000«, © Landesvermessungsamt Schleswig-Holstein. The following map sheets were used:

L 2124 Bad Bramstedt (2003), L 2324 Pinneberg (2003)

The map has a digitally constructed border and tick marks indicating coordinates in the Gauss-Krüger coordinate system. The grey-shading of the topography of the thematic map has a screen density of 50% of the original digital topographic map.

5.2. Flight-Line Maps

The flight-line maps show the position of the surveyed profiles on the topographic maps. The corresponding line number is shown at the end of a profile at which the flight for that profile commenced. Positions of selected time marks (records), e.g., every 100th, are marked with an “×”. Every tenth plotted time mark is labelled with its number. The flight-line maps permit fast and easy correlation of data from profiles and vertical sections and their position in the survey area.

5.3. Thematic Maps

Geophysical thematic maps (**Table 20**) were produced for all survey areas, together with the topography. Each of the maps has a detailed legend which contains information about the survey area, the base maps, the scale, the plotted geophysical parameter(s), and the people participating and institutions.

5.4. Digital Elevation Models

Digital elevation models (DEM) can be derived from the altitude of the HEM bird minus the laser altitude of the bird. The bird altitude is obtained directly from the DGPS-Z readings or – if the DGPS-Z data is not available – from the barometric altitude of the helicopter minus the effective cable length, i.e., the distance of the HEM bird from the helicopter.

6. Archiving

All data sets and plots are stored on CD-ROMs and archived at BGR section B 3.13 – Applied Airborne and Ground Geophysics. The data formats of processed data are described in **Appendix II**. A technical report, the vertical sections, and the thematic maps (as PDF files) are stored together with the final data (ASCII-coded in GEOSOFT-XYZ format) on CD-ROM **Table 20**). This report encloses a copy of the CD-ROM listed in **Appendix III**. **Appendix IV** and **Appendix V** contain copies of all maps and vertical resistivity sections, respectively, reduced to smaller scales fitting the A4 format of this report.

Table 20: *Contents of the CD-ROM*

Directory		Description of contents
\Adobe Acrobat		Adobe® Acrobat Reader in diverse versions for popular system software
\Report		Technical report of the project in PDF format
\Data…	\HEM	ASCII file with all processed data (*.dat) ASCII file with all derived parameters (*.app) ASCII file with starting models for the 1-D inversion (*.sta) ASCII file with results of the 1-D inversion (*.inv) ASCII file with synthetic data derived from the 1-D inversions (*.syn)
	\MAG	ASCII file with data of the total magnetic field, IGRF, base station data, diurnal variations etc.
	\SCI	ASCII file with data of the equivalent concentrations of potassium, uranium and thorium and the total radiation
\Maps…	\HEM	Half-space resistivity maps and centroid depth maps at a scale of 1:50,000 for the frequencies 387.2 Hz, 1820 Hz, 8225 Hz, 41,550 Hz, 133,200 Hz in PDF format Resistivity maps and depth maps at a scale of 1:50,000 for layers 2–5 based on five-layer inversion results in PDF format Resistivity maps at a scale of 1:50,000 at 0, 5, 10, 15, 20, 25, 30, 35, 40, 45, 50, 55, 60, 65, and 70 m below mean sea level based on five-layer inversion results in PDF format
	\MAG	Magnetic anomalies map at a scale of 1:50,000 in PDF format
	\SCI	Maps of the equivalent concentrations of the radio elements potassium, uranium, and thorium, the total radiation and the ground level exposure rate at a scale of 1:50,000 in PDF format
	\Flight lines	Flight line map with topography at a scale of 1:50,000 in PDF format
	\DEM	Digital elevation model at a scale of 1:50 ,000 in PDF format
\Vertical sections		Vertical resistivity section based on five-layer inversion results for each profile of the survey area at a horizontal scale of 1:50,000 and at a vertical scale of 1:5000 in PDF format

7. Personnel

Field Crew

Hans-Joachim **Rehli**, management and system engineering, B3.13, BGR
Karl-Heinz **Meinhardt**, system operation and engineering, B3.13, BGR
Josef **Scheiwein**, helicopter engineering, B3.13, BGR
Michael **Schütt**, pilot, Wiking Helikopter Service GmbH
Hanno **Schmidt**, navigation and field data processing, B3.13, BGR
Wolfgang **Voß**, navigation and field data processing, B3.13, BGR

Office Crew

Dr. Uwe **Meyer**, head of section B3.13, BGR
Dr. Bernhard **Siemon**, HEM data evaluation, B3.13, BGR
Dr. Detlef **Eberle**, radiometric data evaluation, B3.13, BGR
Wolfgang **Voß**, magnetic data evaluation, B3.13, BGR
Jens **Pielawa**, cartographic work, B3.13, BGR

Address: Federal Institute for Geosciences and Natural Resources (BGR)
Stilleweg 2
30655 Hannover
Germany
Tel.: +49 511 643 3212 (Meyer)
3238 (Rehli)
3488 (Siemon)
Fax: +49 511 643 3663
Email: heli@bgr.de, u.meyer@bgr.de, b.siemon@bgr.de, h-j.rehli@bgr.de

8. References

Boulton, G. S. & Caban, P. 1995. Groundwater flow beneath ice sheets: Part II – Its impact on glacier structures and moraine formation. *Quaternary Science Reviews*, **14**, 6, 563-587.

Boulton, G. S., Caban, P. E. & Gijssel, K. V. 1995. Groundwater flow beneath ice sheets: Part I – Large scale patterns. *Quaternary Science Reviews*, **14**, 6, 545-562.

Gausland, A. K. 1998. *Distribution and genesis of Late Pleistocene buried channels in the central North Sea*. Cand. Scient Thesis, University of Oslo.

IAGA, 1992: International Geomagnetic Reference Field, 1991 Revision. International Association of Geomagnetism and Aeronomy (IAGA) Division V, Working Group 8: Analysis of the main field and secular variation. Geophys. J. Int., 108, 945–946.

IAEA, 1979: Gamma-ray surveys in Uranium exploration. Technical Report Series no. 186, International Atomic Energy Agency, Vienna.

IAEA, 1991: Airborne gamma-ray spectrometer surveying. Technical Report Series no. 323, International Atomic Energy Agency, Vienna.

Huuse, M. & Lykke-Andersen, H. 2000. Overdeepended Quaternary valleys in the eastern Danish North Sea: morphology and origin. *Quaternary Science Review*, **19**, 1233-1253.

Huuse, M., Lykke-Andersen, H. and Piotrowski, J. A., 2003. Geophysical Investigations of Buried Quaternary Valleys in the Formerly Glaciated NW European Lowland: Significance for Groundwater Exploration. *Journal of Applied Geophysics*, **53**, No.4, 153-300.

Sengpiel, K.-P. & Siemon, B., 2000. Advanced inversion methods for airborne electromagnetic exploration. Geophysics, 65, 1983–1992.

Siemon, B., 2001: Improved and new resistivity-depth profiles for helicopter electromagnetic data. J. Appl. Geophys., 46, 65–76.

BUNDESANSTALT FÜR GEOWISSENSCHAFTEN UND ROHSTOFFE

BGR, HANNOVER

i. V.

(Dr. H.-R. Kudraß)

Director and Professor
Division
"Geophysics,
Marine and Polar Research"

(Dr. B. Siemon)

Section
"Applied Airborne and
Ground Geophysics"

Appendix I

Ellerbeker Rinne – Survey 2005

Flight	Date	Time (UTC) Start – End	Lines	Remarks
11100	19.04.05	09:08 – 11:16	115.1 W 118.1 E 121.1 W 124.1 E 127.1 W 130.1 E 133.1 W 136.1 E 139.1 W 142.1 E 143.1 W 144.1 E 112.1 W 109.1 E	**Basis: Airport Hartenholm** **Airport elevation: 32 m** **EM: Bird BKS 60** **EM:** noise in the highest frequency (128.5 kHz) during the whole flight Line 112.1, Fid 672 - 680: strong noise in EM and Mag due to a radio transmitter Weather: clouded, rain, 5° C, wind from 70° with 10 to 16 knots **Profile kilometres:** 80
11101	19.04.05	15:11 – 17:07	1.9 S 2.9 N 3.9 S 4.9 N 5.9 S 6.9 N	**Basis: Airport Hartenholm** **Cross Profiles** **EM:** noise in the highest frequency (128.5 kHz) during the whole flight Weather: sunny, 12° C **Profile kilometres:** 136
11102	20.04.05	07:41 – 09:46	106.1 E 103.1 W 100.1 E 97.1 W 94.1 E 91.1 W 88.1 E 85.1 W 82.1 E 79.1 W 76.1 E 73.1 W 70.1 E	**Basis: Airport Hartenholm** **EM:** noise in the highest frequency (128.5 kHz) during the whole flight Line 70.1: oscillation of the 4th frequency right from the beginning of the line Weather: sunny, wind from 10° with 20 knots, 12° C **Profile kilometres:** 84

Ellerbeker Rinne – Survey 2006

Flight	Date	Time (UTC) Start – End	Lines	Remarks
11103	16.05.06	13:43 – 15:51	201.1 W 202.1 E 203.1 W 204.1 E 205.1 W 206.1 E 207.1 W 208.1 E 209.1 W 210.1 E 211.1 W 212.1 E 213.1 W 214.1 E	**Basis: Airport Hartenholm** **Airport elevation: 32 m** **Coordinates of the magnetic base station:** 53.9164810° N; 10.0352259° E **EM: Bird BKS 36a** Weather: clouded, occasionally rain, 12° C, strong wind with 20 to 25 knots **Profile kilometres:** 168
11104	17.05.06	07:39 – 10:08	215.1 W 216.1 E 217.1 W 218.1 E 219.1 W 220.1 E 221.1 W 222.1 E 223.1 W 224.1 E 225.1 W 226.1 E 227.1 W 228.1 E 229.1 W 230.1 E 231.1 W 232.1 E	**Basis: Airport Hartenholm** Weather: clouded, 10° C, wind with 5 knots from 300° **Profile kilometres:** 211

Flight	Date	Time (UTC) Start – End	Lines	Remarks
11105	17.05.06	11:42 – 13:59	272.1 E 271.1 W 270.1 E 269.1 W 268.1 E 267.1 W 266.1 E 265.1 W 264.1 E 263.1 W 262.1 E 261.1 W 260.1 E 259.1 W 258.1 E 257.1 W 256.1 E 255.1 W 254.1 E 253.1 W 252.1 E 251.1 W 250.1 E	**Basis: Airport Hartenholm** Weather: clouded, 16° C, moderate wind **Profile kilometres:** 129
11106	18.05.06	11:46 – 12:48	249.1 W 248.1 E 247.1 W 246.1 E 245.1 W 244.1 E 243.1 W 242.1 E	Weather: clouded, 13° C, strong wind with 15 to 28 knots Stop of the survey flight after line 242.1; Q-coil anomalies can't be switched on. **Profile kilometres:** 56

Flight	Date	Time (UTC) Start – End	Lines	Remarks
11107	18.06.05	13:36 – 14:45	241.1 W 240.1 E 239.1 W 238.1 E 239.1 W 238.1 E 237.1 W 236.1 E 235.1 W 234.1 E 233.1W 232.2 E	Weather: sunny, 21° C, strong wind with 20 knots **Profile kilometres:** 77

Appendix II

Final Data Format Description

Electromagnetics

Description of the five ASCII-coded data files containing the final (leveled) data of a helicopter-borne electromagnetic (HEM) survey

Gereral HEADER:

```
/BGR HEADER (SHORT VERSION):
/
/AREANAME
/Ellerbek
/AREACODE
/111
/C_MERIDIAN, ZONE AND GEOID
/  9  3 BESSEL
/BIRD
/61
/NUMFREQ
/ 5
/FREQUENCY
/    375.00   1778.00   8510.00  37830.00 128500.00        (system parameters of the 2005 survey)
/    387.20   1820.00   8210.00  41550.00 133200.00        (system parameters of the 2006 survey)
/COILSEPERATION
/      7.92      7.91      7.96      8.03      7.92         (system parameters of the 2006 survey)
/      7.94      7.93      7.93      7.91      7.92         (system parameters of the 2006 survey)
/COILGEOMETRY (1 = hor. copl.)
/      1.00      1.00      1.00      1.00      1.00
/TOWCABLE
/ 37.00
/DUMMY
/    9999.990
/DECIMATIONVALUE
/ 1
/PRIVTEXT
/programm: hem05
/BERECHNETE HALBRAUMPARAMETER
/PROGRAMM: HEM_KOR05
/KORRIGIERTE DATEN VON  E:\SIEMONB\GEBIETE\111_ELLERBEKER-RINNE\KOR\HEM1110019DAT.XYZ
/UEBERTRAGEN AM  19-JUN-06 17:39:34
```

DATA:

'xxx' internal area number: 112 for Ellerbeker Rinne

1) HEM'xxx'_dat.xyz :

Example:

/	X	Y	RECORD	TOPO	H_RADAR	H_LASER	BIRD_NN	H_BARO	REAL_1	QUAD_1	REAL_2	QUAD_2	REAL_3	QUAD_3	REAL_4	QUAD_4	REAL_5	QUAD_5
TIE	1.9																	
	545408	5968554	14950	8.02	59.12	59.81	58.99	73.94	29.07	36.05	69.49	78.34	177.52	140.83	323.98	129.62	429.56	86.06
	545410	5968551	14951	8.00	59.61	59.79	58.92	73.84	29.10	36.10	69.71	78.00	177.69	141.32	324.94	130.77	431.60	87.39
	545412	5968548	14952	7.97	58.88	59.67	58.86	73.75	29.11	36.14	69.79	77.66	177.83	141.75	325.83	131.86	433.49	88.69

lines beginning with '/' are comment lines
lines beginning with 'LINE' mark the beginning of a new profile line
lines beginning with 'TIE' mark the beginning of a new tie line (cross-flown)

In this data file all measured parameters are stored in the order of the following description:

X = Gauß-Krüger easting in m (Zone 3), these coordinates have a false easting of 3000000 metres.
Y = Gauß-Krüger northing in m (Zone 3), these coordinates have no false northing.
RECORD = time mark increasing by 1 every 0.1 seconds.
TOPO = topographic elevation (in metre above sea level).
H_RADAR = smoothed value of the radar altitude (in metre) minus the effective cable length (37 metre) from the helicopter to the bird; corresponds to the bird altitude in metre above ground level.
H_LASER = smoothed value of the laser altimeter (in metre); corresponds to the bird altitude in metre above ground level.
BIRD_NN = smoothed bird altitude (in m a.m.s.l. = metre above mean sea level).
H_BARO = filtered value of the barometric sensor (in metre) minus the effective cable length (37 metre) from the helicopter to the bird; corresponds to the bird altitude (in metre above mean sea level).
REAL_1 = filtered value (in ppm) of the inphase component at the frequency f = 387.2 (375) Hz.
QUAD_1 = filtered value (in ppm) of the out-of-phase component at the frequency f = 387.2 (375) Hz
REAL_2 = filtered value (in ppm) of the inphase component at the frequency f = 1820 (1778) Hz
QUAD_2 = filtered value (in ppm) of the out-of-phase component at the frequency f = 1820 (1778) Hz
REAL_3 = filtered value (in ppm) of the inphase component at the frequency f = 8225 (8510) Hz
QUAD_3 = filtered value (in ppm) of the out-of-phase component at the frequency f = 8225 (8510) Hz
REAL_4 = filtered value (in ppm) of the inphase component at the frequency f = 41550 (37830) Hz
QUAD_4 = filtered value (in ppm) of the out-of-phase component at the frequency f = 41550 (37830) Hz
REAL_5 = filtered value (in ppm) of the inphase component at the frequency f = 133200 (128500) Hz
QUAD_5 = filtered value (in ppm) of the out-of-phase component at the frequency f = 133200 (128500) Hz

2) HEM'xxx'_app.xyz :

Example:

/	X	Y	RECORD	TOPO	H_RADAR	H_LASER	BIRD_NN	H_BARO	RHOA_1	KDA_1	ZST_1	RHOA_2	KDA_2	ZST_2	RHOA_3	KDA_3	ZST_3	RHOA_4	KDA_4	ZST_4	RHOA_5	KDA_5	ZST_5
TIE	1.9																						
	545408	5968554	14950	8.02	59.12	59.81	58.99	73.94	15.83	21.74	73.44	37.17	5.19	41.58	57.77	-1.71	19.02	52.63	-0.03	9.36	39.78	0.32	4.75
	545410	5968551	14951	8.00	59.61	59.79	58.92	73.84	15.83	21.71	73.42	36.74	5.46	41.64	57.95	-1.78	18.98	53.10	-0.14	9.28	40.47	0.19	4.66
	545412	5968548	14952	7.97	58.88	59.67	58.86	73.75	15.84	21.79	73.50	36.44	5.80	41.82	58.13	-1.74	19.06	53.56	-0.15	9.32	41.18	0.17	4.67

lines beginning with '/' are comment lines
lines beginning with 'LINE' mark the beginning of a new profile line
lines beginning with 'TIE' mark the beginning of a new tie line (cross-flown)

In this data file all necessary measured parameters as well as the calculated parameters rhoa, da and zstern are stored in the order of the following description:

X = Gauß-Krüger easting in m (Zone 3), DHDN system(Bessel-Ellipsoid), these coordinates have a false easting of 3000000 metres.
Y = Gauß-Krüger northing in m (Zone 3), DHDN system(Bessel-Ellipsoid), these coordinates have no false northing.
RECORD = time mark increasing by 1 every 0.1 seconds.
TOPO = topographic elevation (in metre above sea level).
H_RADAR = smoothed value of the radar altitude (in metre) minus the effective cable length (37 metre) from the helicopter to the bird; corresponds to the bird altitude in metre above ground level.
H_LASER = smoothed value of the laser altimeter (in metre); corresponds to the bird altitude in metre above ground level.
BIRD_NN = smoothed bird altitude (in m a.m.s.l. = metre above mean sea level).
H_BARO = filtered value of the barometric sensor (in metre) minus the effective cable length (37 metre) from the helicopter to the bird; corresponds to the bird altitude (in metre above mean sea level).
RHOA_1 = apparent resistivity (in Ohm*m) at the frequency f = 387.2 (375) Hz
KDA_1 = apparent depth (in metre) of the ground level to the top of the conductive half-space at the frequency f = 387.2 (375) Hz
ZST_1 = centroid depth (in metre) at the frequency f = 387.2 (375) Hz
RHOA_2 = apparent resistivity (in Ohm*m) at the frequency f = 1820 (1778) Hz
KDA_2 = apparent depth (in metre) of the ground level to the top of the conductive half-space at the frequency f = 1820 (1778) Hz
ZST_2 = centroid depth (in metre) at the frequency f = 1820 (1778) Hz
RHOA_3 = apparent resistivity (in Ohm*m) at the frequency f = 8225 (8510) Hz
KDA_3 = apparent depth (in metre) of the ground level to the top of the conductive half-space at the frequency f = 8225 (8510) Hz
ZST_3 = centroid depth (in metre) at the frequency f = 8225 (8510) Hz
RHOA_4 = apparent resistivity (in Ohm*m) at the frequency f = 41550 (37830) Hz
KDA_4 = apparent depth (in metre) of the ground level to the top of the conductive half-space at the frequency f = 41550 (37830) Hz
ZST_4 = centroid depth (in m) at the frequency f = 41550 (37830) Hz
RHOA_5 = apparent resistivity (in Ohm*m) at the frequency f = 133200 (128500) Hz
KDA_5 = apparent depth (in metre) of the ground level to the top of the conductive half-space at the frequency f = 133200 (128500) Hz
ZST_5 = centroid depth (in metre) at the frequency f = 133200 (128500) Hz

3) HEM'xxx'_sta.xyz :

Example:

```
/     X        Y      RECORD  TOPO  H_RADAR  H_LASER  BIRD_NN  H_BARO  RHO_S_1  D_S_1  RHO_S_2  D_S_2  RHO_S_3  D_S_3  RHO_S_4  D_S_4  RHO_S_5
TIE   1.9
  545408  5968554  14950   8.02   59.12    59.81    58.99    73.94  5000.00  0.82   45.75    12.52  57.77    14.78  37.17    27.14  15.83
  545410  5968551  14951   8.00   59.61    59.79    58.92    73.84  5000.00  0.69   46.36    12.58  57.96    14.84  36.74    27.17  15.83
  545412  5968548  14952   7.97   58.88    59.67    58.86    73.75  5000.00  0.67   46.96    12.65  58.13    14.91  36.45    27.21  15.84
```

lines beginning with '/' are comment lines
lines beginning with 'LINE' mark the beginning of a new profile line
lines beginning with 'TIE' mark the beginning of a new tie line (cross-flown)

In this data file all necessary measured parameters as well as the starting model parameters for the 1D-Inversion rho and d are stored in the order of the following description:

X = Gauß-Krüger easting in m (Zone 3), DHDN system(Bessel-Ellipsoid), these coordinates have a false easting of 3000000 metres.
Y = Gauß-Krüger northing in m (Zone 3), DHDN system(Bessel-Ellipsoid), these coordinates have no false northing.
RECORD = time mark increasing by 1 every 0.1 seconds.
TOPO = topographic elevation (in metre above sea level).
H_RADAR = smoothed value of the radar altitude (in metre) minus the effective cable length (37 metre) from the helicopter to the bird; corresponds to the bird altitude in metre above ground level.
H_LASER = smoothed value of the laser altimeter (in metre); corresponds to the bird altitude in metre above ground level.
BIRD_NN = smoothed bird altitude (in m a.m.s.l. = metre above mean sea level).
H_BARO = filtered value of the barometric sensor (in metre) minus the effective cable length (37 metre) from the helicopter to the bird; corresponds to the bird altitude (in metre above mean sea level).
RHO_S_1 = resistivity (in Ohm*m) of the first (top) layer of a five-layer starting model
D_S_1 = thickness (in metre) of the first (top) layer of a five-layer starting model
RHO_S_2 = resistivity (in Ohm*m) of the second layer of a five-layer starting model
D_S_2 = thickness (in metre) of the second layer of a five-layer starting model
RHO_S_3 = resistivity (in Ohm*m) of the third layer of a five-layer starting model
D_S_3 = thickness (in metre) of the third layer of a five-layer starting model
RHO_S_4 = resistivity (in Ohm*m) of the fourth layer of a five-layer starting model
D_S_4 = thickness (in metre) of the fourth layer of a five-layer starting model
RHO_S_5 = resistivity (in Ohm*m) of the fifth layer of a five-layer inversion model

4) HEM'xxx'_inv.xyz :

Example:

/	X	Y	RECORD	TOPO	H_RADAR	H_LASER	BIRD_NN	H_BARO	RHO_I_1	D_I_1	RHO_I_2	D_I_2	RHO_I_3	D_I_3	RHO_I_4	D_I_4	RHO_I_5	QALL
TIE	1.9																	
	545408	5968554	14950	8.02	59.12	59.81	58.99	73.94	5033.38	1.26	41.47	7.69	59.04	13.21	45.80	43.32	10.81	3.98
	545410	5968551	14951	8.00	59.61	59.79	58.92	73.84	5033.77	1.11	42.25	7.69	59.10	13.11	45.45	44.34	10.39	3.92
	545412	5968548	14952	7.97	58.88	59.67	58.86	73.75	5032.17	1.05	43.17	8.00	59.30	13.26	45.32	43.89	10.26	3.79

lines beginning with '/' are comment lines
lines beginning with 'LINE' mark the beginning of a new profile line
lines beginning with 'TIE' mark the beginning of a new tie line (cross-flown)

In this data file all necessary measured parameters as well as the results of a 1D-Inversion rho, d and qall are stored in the order of the following description:

X = Gauß-Krüger easting in m (Zone 3), DHDN system(Bessel-Ellipsoid), these coordinates have a false easting of 3000000 metres.
Y = Gauß-Krüger northing in m (Zone 3), DHDN system(Bessel-Ellipsoid), these coordinates have no false northing.
RECORD = time mark increasing by 1 every 0.1 seconds.
TOPO = topographic elevation (in metre above sea level).
H_RADAR = smoothed value of the radar altitude (in metre) minus the effective cable length (37 metre) from the helicopter to the bird; corresponds to the bird altitude in metre above ground level.
H_LASER = smoothed value of the laser altimeter (in metre); corresponds to the bird altitude in metre above ground level.
BIRD_NN = smoothed bird altitude (in m a.m.s.l. = metre above mean sea level).
H_BARO = filtered value of the barometric sensor (in metre) minus the effective cable length (37 metre) from the helicopter to the bird; corresponds to the bird altitude (in metre above mean sea level).
RHO_I_1 = resistivity (in Ohm*m) of the first (top) layer of a five-layer inversion model
D_I_1 = thickness (in mere) of the first (top) layer of a five-layer inversion model
RHO_I_2 = resistivity (in Ohm*m) of the second layer of a five-layer inversion model
D_I_2 = thickness (in metre) of the second layer of a five-layer inversion model
RHO_I_3 = resistivity (in Ohm*m) of the third layer of a five-layer inversion model
D_I_3 = thickness (in metre) of the third layer of a five-layer inversion model
RHO_I_4 = resistivity (in Ohm*m) of the fourth layer of a five-layer inversion model
D_I_4 = thickness (in metre) of the fourth layer of a five-layer inversion model
RHO_I_5 = resistivity (in Ohm*m) of the fifth layer of a five-layer inversion model

QALL = misfit of the inversion (in percent)

5) **HEM'xxx'_syn.xyz :**

Example:

/ X	Y	RECORD	TOPO	H_RADAR	H_LASER	BIRD_NN	H_BARO	REAL_1	QUAD_1	REAL_2	QUAD_2	REAL_3	QUAD_3	REAL_4	QUAD_4	REAL_5	QUAD_5
TIE 1.9																	
545408	5968554	14950	8.02	59.12	59.81	58.99	73.94	25.70	34.15	67.75	73.77	178.96	133.44	330.42	130.28	425.12	90.33
545410	5968551	14951	8.00	59.61	59.79	58.92	73.84	25.93	34.09	67.75	73.83	179.30	133.78	331.07	131.35	427.17	91.76
545412	5968548	14952	7.97	58.88	59.67	58.86	73.75	26.11	34.14	67.88	73.85	179.44	134.29	332.16	132.50	429.34	93.00

lines beginning with '/' are comment lines
lines beginning with 'LINE' mark the beginning of a new profile line
lines beginning with 'TIE' mark the beginning of a new tie line (cross-flown)

In this data file all synthetic data derived from 1-D inversion models are stored in the order of the following description:

X = Gauß-Krüger easting in m (Zone 3), DHDN system(Bessel-Ellipsoid), these coordinates have a false easting of 3000000 metres.
Y = Gauß-Krüger northing in m (Zone 3), DHDN system(Bessel-Ellipsoid), these coordinates have no false northing.
RECORD = time mark increasing by 1 every 0.1 seconds.
TOPO = topographic elevation (in metre above sea level).
H_RADAR = smoothed value of the radar altitude (in metre) minus the effective cable length (37 metre) from the helicopter to the bird; corresponds to the bird altitude in metre above ground level.
H_LASER = smoothed value of the laser altimeter (in metre); corresponds to the bird altitude in metre above ground level.
BIRD_NN = smoothed bird altitude (in m a.m.s.l. = metre above mean sea level).
H_BARO = filtered value of the barometric sensor (in metre) minus the effective cable length (37 metre) from the helicopter to the bird; corresponds to the bird altitude (in metre above mean sea level).
REAL_1 = inphase component of the model data (in ppm) at the frequency f = 387.2 (375) Hz
QUAD_1 = out-of-phase component of the model data (in ppm) at the frequency f = 387.2 (375) Hz
REAL_2 = inphase component of the model data (in ppm) at the frequency f = 1820 (1778) Hz
QUAD_2 = out-of-phase component of the model data (in ppm) at the frequency f = 1820 (1778) Hz
REAL_3 = inphase component of the model data (in ppm) at the frequency f = 8225 (8510) Hz
QUAD_3 = out-of-phase component of the model data (in ppm) at the frequency f = 8225 (8510) Hz
REAL_4 = inphase component of the model data (in ppm) at the frequency f = 41550 (37830) Hz
QUAD_4 = out-of-phase component of the model data (in ppm) at the frequency f = 41550 (37830) Hz
REAL_5 = inphase component of the model data (in ppm) at the frequency f = 133200 (128500) Hz
QUAD_5 = out-of-phase component of the model data (in ppm) at the frequency f = 133200 (128500) Hz

Dummy value 9999.99

Magnetics

Description of the ASCII-coded data file containing the final (leveled) data of a helicopter-borne magnetic survey

MAG'xxx'.xyz

'xxx' internal area number: 111 for Ellerbeker Rinne

"/" are comment lines
"*" are dummy values

Line 201.1 is the line header for line number 201.1
/ XYZ EXPORT [07/13/2006]
/ DATABASE [.\MAG.gdb]
/

/ X	Y	Lat_WGS_84	Lon_WGS_84	RECORD	Radar	Laser	Bird_NN	Topo	mag_base	Igrf	incli	decli	diurnal	f_mag	delta_T_KORR	delta_T_lev
Line 201.1																
554405	5974590	53.8993565	9.8266068	6197	55.43	56.26	68.50	17.41	49507.00	49447.26	68.67	1.04	7.00	49536.18	80.66	84.956
554402	5974589	53.8993443	9.8265607	6198	54.88	56.09	68.30	17.40	49507.00	49447.26	68.67	1.04	7.00	49536.04	80.56	84.902
554399	5974588	53.8993322	9.8265145	6199	54.36	55.81	68.00	17.40	49507.00	49447.25	68.67	1.04	7.00	49535.95	80.50	84.859

Channel description:

X	Gauß-Krüger easting in m (Zone 3), DHDN system(Bessel-Ellipsoid), these coordinates have a false easting of 3000000 metres
Y	Gauß-Krüger northing in m (Zone 3), DHDN system(Bessel-Ellipsoid)
Lat_WGS_84	Latitude Value (degrees) WGS84 system
Lon_WGS_84	Longitude value (degrees) WGS84 system
RECORD	time mark increasing by 1 every 0.1 seconds
Radar	smoothed value of the radar altitude (in metre) minus the effective cable length (37 metre) from the helicopter to the bird; corresponds to the bird altitude in metre above ground level
LASER	smoothed value of the laser altimeter (in metre); corresponds to the bird altitude in metre above ground level.
BIRD_NN	smoothed bird altitude (in m a.m.s.l. = metre above mean sea level).
TOPO	topographic elevation (in metre above sea level).
mag_base	total field value at mag base station at ground [nT]
Igrf	IGRF value at lat/long value for the altitude of the Bird (bird_NN), Epoch 2006.4 [nT]
incli	inclination of main magnetic field at lat/long value in Degrees
decli	declination of main magnetic field at lat/long value in Degrees
diurnal	diurnal variation at mag base station subtracting mean value [nT]
f_mag	despiked and filtered value of the total magnetic field [nT]
delta_t_korr	heading error corrected value of the total magnetic field and subtraction of Igrf and diurnal variations [nT]
delta_T_lev	leveled value of the anomalous magnetic field [nT]

Radiometrics

Description of the ASCII-coded data file containing the final (leveled) data of a helicopter-borne radiometric survey

SCI'xxx'.xyz

'xxx' internal area number: 111 for Ellerbeker Rinne

lines with "/" are comment lines
line 70.1 line number
tie 1.9 tie line number

```
/ ---------------------------------------------------------------------------
/ XYZ EXPORT [09/14/2006]
/ DATABASE   [.\sci111.gdb]
/ ---------------------------------------------------------------------------
/        X          Y      Lat_WGS_84   on_WGS_84   Record     Radar      Baro      s_tot    c_pot    c_tho    c_ura    tc_expo
/========== ========== ================== ================= ========== ========== ========== ========== ========== ========== ========== ============
/
Line  70.1
   550506   5957223      53.7437063      9.7644468     6285     99.35    101.37    232.69     0.82     2.21     0.52     2.21
   550533   5957240      53.7438600      9.7648518     6286     97.20     99.32    229.71     0.79     2.25     0.53     2.19
   550559   5957258      53.7440158      9.7652542     6287     96.21     97.25    228.27     0.77     2.29     0.53     2.17
```

Channel description:

X	Gauß-Krüger easting in m (Zone 3), DHDN system(Bessel-Ellipsoid), these coordinates have a false easting of 3000000 metres
Y	Gauß-Krüger northing in m (Zone 3), DHDN system(Bessel-Ellipsoid)
Lat_WGS_84	Latitude Value (degrees) WGS84 system
Lon_WGS_84	Longitude value (degrees) WGS84 system
Record	time mark increasing by 1 every second
Radar	smoothed value of the radar altitude (in metre); corresponds to the helicopter altitude in metre above ground level
Baro	filtered value of the barometric sensor (in metre); corresponds to the bird altitude (in metre above mean sea level).
s_tot	stripped total count rate in counts per second [cps]
c_pot	concentration of K40 [%]
c_tho	concentration of Thorium Th [ppm]
c_ura	concentration of Uranium U [ppm]
TC_expo	Total count exposure rate TC_expo [micro Roentgens/h]

Appendix III

CD-ROM

Acrobat Reader\
liesmich.txt
Acrobat Reader\Linux\
AdobeReader_deu-7.0.5-1.i386.tar.gz
Acrobat Reader\Mac\
AdbeRdr708_de_DE.dmg
Acrobat Reader\Win 3.1\
rs16d301.exe
Acrobat Reader\Win 95\
rp505deu.exe
Acrobat Reader\Win NT\
AdbeRdr708_DLM_de_DE.exe
Acrobat Reader\Win XP\
AdbeRdr708_DLM_de_DE.exe

Data\
Data\HEM\
HEM111_APP.xyz
HEM111_DAT.xyz
HEM111_INV.xyz
HEM111_STA.xyz
HEM111_SYN.xyz
readme_hem.txt
Data\MAG\
MAG111.xyz
readme_mag.txt
Data\SCI\
readme_sci.txt

Maps\
Maps\DEM\
TK50 Ellerbeker Rinne DEM.pdf
Maps\Flight lines\
TK50 Ellerbeker Rinne Flight lines.pdf
Maps\HEM\
TK50 Ellerbeker Rinne resistivity -00m.pdf
TK50 Ellerbeker Rinne resistivity -05m.pdf
TK50 Ellerbeker Rinne resistivity -10m.pdf
TK50 Ellerbeker Rinne resistivity -15m.pdf
TK50 Ellerbeker Rinne resistivity -20m.pdf
TK50 Ellerbeker Rinne resistivity -25m.pdf
TK50 Ellerbeker Rinne resistivity -30m.pdf
TK50 Ellerbeker Rinne resistivity -35m.pdf
TK50 Ellerbeker Rinne resistivity -40m.pdf
TK50 Ellerbeker Rinne resistivity -45m.pdf
TK50 Ellerbeker Rinne resistivity -50m.pdf
TK50 Ellerbeker Rinne resistivity -55m.pdf
TK50 Ellerbeker Rinne resistivity -60m.pdf
TK50 Ellerbeker Rinne resistivity -65m.pdf
TK50 Ellerbeker Rinne resistivity -70m.pdf
TK50 Ellerbeker Rinne resistivity rho2.pdf
TK50 Ellerbeker Rinne resistivity rho3.pdf
TK50 Ellerbeker Rinne resistivity rho4.pdf
TK50 Ellerbeker Rinne resistivity rho5.pdf
TK50 Ellerbeker Rinne rhoa1.pdf
TK50 Ellerbeker Rinne rhoa2.pdf
TK50 Ellerbeker Rinne rhoa3.pdf
TK50 Ellerbeker Rinne rhoa4.pdf
TK50 Ellerbeker Rinne rhoa5.pdf
TK50 Ellerbeker Rinne upper boundary z2.pdf
TK50 Ellerbeker Rinne upper boundary z3.pdf
TK50 Ellerbeker Rinne upper boundary z4.pdf
TK50 Ellerbeker Rinne upper boundary z5.pdf
TK50 Ellerbeker Rinne zst1.pdf
TK50 Ellerbeker Rinne zst2.pdf
TK50 Ellerbeker Rinne zst3.pdf
TK50 Ellerbeker Rinne zst4.pdf
TK50 Ellerbeker Rinne zst5.pdf
Maps\MAG\
TK50 Ellerbeker Rinne Anomalies of the magnetic field.pdf
Maps\SCI\
TK50 Ellerbeker Rinne Exposure rate.pdf
TK50 Ellerbeker Rinne Potassium.pdf
TK50 Ellerbeker Rinne Thorium.pdf
TK50 Ellerbeker Rinne Total count.pdf
TK50 Ellerbeker Rinne Uranium.pdf

Report\
Technical report BurVal Ellerbeker Rinne.pdf

Vertical sections\
VRS 1110018.pdf
VRS 1110019.pdf
VRS 1110028.pdf
VRS 1110029.pdf
VRS 1110038.pdf
VRS 1110039.pdf
VRS 1110048.pdf
VRS 1110049.pdf
VRS 1110059.pdf
VRS 1110069.pdf
VRS 1110701.pdf

VRS 1110731.pdf
VRS 1110761.pdf
VRS 1110791.pdf
VRS 1110821.pdf
VRS 1110851.pdf
VRS 1110881.pdf
VRS 1110911.pdf
VRS 1110941.pdf
VRS 1110971.pdf
VRS 1110972.pdf
VRS 1111001.pdf
VRS 1111031.pdf
VRS 1111061.pdf
VRS 1111091.pdf
VRS 1111121.pdf
VRS 1111151.pdf
VRS 1111181.pdf
VRS 1111211.pdf
VRS 1111212.pdf
VRS 1111241.pdf
VRS 1111242.pdf
VRS 1111271.pdf
VRS 1111272.pdf
VRS 1111301.pdf
VRS 1111331.pdf
VRS 1111332.pdf
VRS 1111361.pdf
VRS 1111391.pdf
VRS 1111421.pdf
VRS 1111431.pdf
VRS 1111432.pdf
VRS 1111441.pdf
VRS 1111442.pdf
VRS 1112011.pdf
VRS 1112021.pdf
VRS 1112031.pdf
VRS 1112041.pdf
VRS 1112051.pdf
VRS 1112061.pdf
VRS 1112071.pdf
VRS 1112081.pdf
VRS 1112091.pdf
VRS 1112101.pdf
VRS 1112111.pdf
VRS 1112121.pdf
VRS 1112131.pdf
VRS 1112141.pdf
VRS 1112151.pdf
VRS 1112161.pdf
VRS 1112171.pdf
VRS 1112181.pdf
VRS 1112191.pdf
VRS 1112201.pdf
VRS 1112211.pdf
VRS 1112221.pdf
VRS 1112231.pdf
VRS 1112241.pdf
VRS 1112251.pdf
VRS 1112261.pdf
VRS 1112271.pdf
VRS 1112281.pdf
VRS 1112291.pdf
VRS 1112301.pdf
VRS 1112311.pdf
VRS 1112321.pdf
VRS 1112322.pdf
VRS 1112331.pdf
VRS 1112341.pdf
VRS 1112351.pdf
VRS 1112361.pdf
VRS 1112371.pdf
VRS 1112381.pdf
VRS 1112391.pdf
VRS 1112401.pdf
VRS 1112411.pdf
VRS 1112421.pdf
VRS 1112431.pdf
VRS 1112441.pdf
VRS 1112451.pdf
VRS 1112461.pdf
VRS 1112471.pdf
VRS 1112481.pdf
VRS 1112491.pdf
VRS 1112501.pdf
VRS 1112511.pdf
VRS 1112521.pdf
VRS 1112531.pdf
VRS 1112541.pdf
VRS 1112551.pdf
VRS 1112561.pdf
VRS 1112571.pdf
VRS 1112581.pdf
VRS 1112591.pdf
VRS 1112601.pdf
VRS 1112611.pdf
VRS 1112621.pdf
VRS 1112631.pdf
VRS 1112641.pdf
VRS 1112651.pdf
VRS 1112661.pdf
VRS 1112671.pdf
VRS 1112681.pdf
VRS 1112691.pdf
VRS 1112701.pdf
VRS 1112711.pdf
VRS 1112721.pdf

Appendix IV
Maps

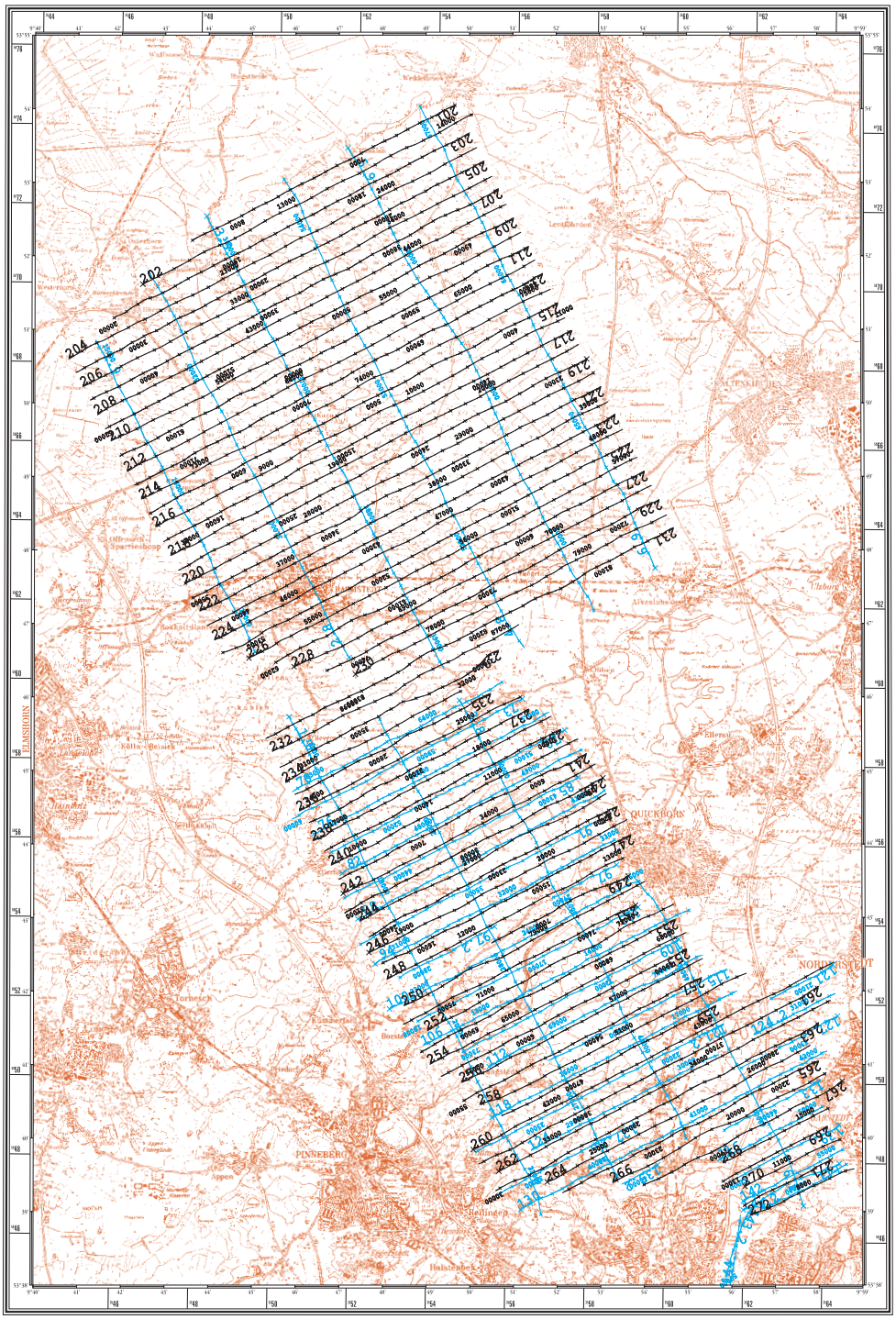

ANCIENT GROUNDWATER RESERVOIRS IN BURIED VALLEYS (BURVAL) – SUSTAINABLE WATER RESOURCES FOR THE FUTURE

The project is co-financed by the European Union

AIRBORNE GEOPHYSICAL SURVEY ELLERBEKER RINNE / GERMANY

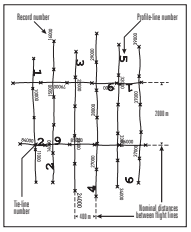

Tick marks indicated in the margin show **Gauß-Krüger-coordinates, Bessel Ellipsoid**. The topography was assembled by the following **base maps 1:50.000:**

L 2124 Bad Bramstedt (1'03)
L 2324 Pinneberg (1'03)

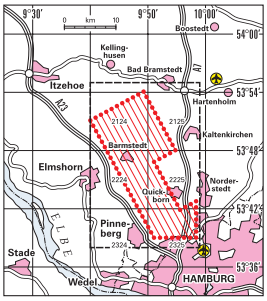

Scale 1:50 000 (2 cm ≙ 1 km)

0 1 2 3 4 5 6 km

Bundesanstalt für Geowissenschaften und Rohstoffe (BGR)
Hannover, Federal Republic of Germany

Landesamt für Natur und Umwelt Schleswig-Holstein (LANU)
Flintbek, Federal Republic of Germany

Behörde für Stadtentwicklung und Umwelt (BSU)
Hamburg, Federal Republic of Germany

Area: **Ellerbeker Rinne**

Parameter: **Topography and flight lines**

Field operation and processing: **April 2005 and May 2006.**
Karl-Heinz Marchardt, Uwe Meyer, Jens Pielawa, Hans-Joachim Rehli, Josef Scheiwein, Hannes Schmidt, Bernhard Siemon, Wolfgang Voß, Michael Schütte (Wilking Helikopter Service GmbH)

B 3.13 · Applied Airborne and Ground Geophysics
Hannover 2006 · www.burval.org · heli@bgr.de

Alle anderen Karten und Vertikal-
sektionen sind in dieser Web-Fassung
des Berichtes nicht enthalten.

All other maps and vertical
resistivity sections are not included
in this web edition of the report.